The Solar-Propulsive Interplanetary Re-supplier

Paul W. Joiner IV[1], Tyler J. Lanes[2], Drake A. Noel[3], Sarah L. Smallwood[4], and Zackary D. Wood[5],
and Daniel White[6]

Arizona State University, Tempe, Arizona, 85281, United States

This document proposes the design of a solar electric propulsion (SEP) space tug, named SPrIntR, that produces 200 kW of power at beginning of life (BOL) for transferring payloads between Low Earth Orbit (LEO) and a Lunar Distant-Retrograde Orbit (LDRO). This design concept is extensible to 500 kW for deep space missions such as excursions from LEO to a Martian Orbit. The decisions and rationale behind each subsystem's design choices are presented. The spacecraft subsystems include power, propulsion, structures and mechanisms, attitude determination and control (AD&C), guidance and navigation (GN), telecommunications, and thermal. Budgets consisting of delta-v, power, mass, momentum, and cost are derived some of which can be traced back to either the top-level or subsystem-level requirements. Additional problem specific design solutions are presented including eclipses and changing power schedule, Xenon propellant sourcing, and component replacement.

I. Nomenclature

A = area, m^2
a = Earth's albedo = 0.3
B = magnetic field strength, T; bandwidth, Hz
B_a = bus contact area, m^2
B_h = bus height, m
B_l = bus length, m
B_m = beam moment, Nm
B_t = bus thickness, m
B_w = bus width, m
C = thermal capacity, W/K
C_d = drag coefficient
C_{nk} = Nextel & Kevlar coefficient
C_p = specific heat capacity, J/[kg-K]
c = speed of light, m/s
D = diameter, m; residual dipole, A-m^2
D_D = docking ring diameter, m
d = distance, diameter, m
d_r = receive antenna diameter, m
d_{SC} = onboard spacecraft antenna diameter, m
d_t = transmit antenna diameter, m
E = Young's modulus, GPa
F = force, N; view factor
f = eclipse fraction; frequency, Hz (structures)/GHz (communications)
g = gravitational acceleration = 9.81 m/s^2
h = height, m; altitude, m

[1-5] Undergraduate Student, Mechanical and Aerospace Engineering, School of Engineering of Matter, Transport & Energy

[6] Lecturer, Mechanical and Aerospace Engineering, School of Engineering, Matter, Transport & Energy

I_{sp}	=	specific impulse, s
i	=	inclination, rad; angle of incidence, rad
J	=	polar moment of inertia, m^4
k	=	thermal conductance, W/[m-K]; Boltzmann's constant
L	=	thickness, m
M, m	=	mass, kg
M_{nk}	=	Nextel & Kevlar areal density, kg/m^2
$\dot{m}$	=	mass flow rate, kg/s
P	=	pressure, Pa; Power, W
P_m	=	Payload mass, kg
Q	=	heat energy, W
Q_{env}	=	solar heat due to albedo, infrared, solar flux
Q_{IR}	=	heat due to Earth's infrared, W
Q_{leak}	=	heat leak into MLI blanket, W
Q_{rad}	=	heat energy from radiation, W
q_e	=	energy flux at Earth = 237 W/m^2
R	=	orbital radius, m; data rate, bps
r	=	radius, m-
S	=	tensile stress, Pa; whipple shield spacing, m; propagation path length, m-
T	=	thrust, N; orbital period, s; torque, N-m; temperature, K; Torsion, Nm
t	=	thickness, m; time, s -
V	=	velocity, m/s
w	=	width, m
α	=	angular acceleration, rad/s^2; surface absorptivity
β	=	factor of safety; beta angle, rad
Δ	=	change in quantity
η	=	efficiency
ε	=	obliquity of the ecliptic, rad; surface emissivity
Γ	=	ecliptic true solar longitude, rad
μ	=	viscosity, N-s/m^2; standard gravitational parameter, m^3/s^2
Ω	=	right ascension of the ascending node
ω	=	angular velocity, rad/s
Ψ	=	transportation rate, kg/day -
ρ	=	density, kg/m^3
σ	=	yield strength, Pa; Stefan-Boltzmann constant = $5.67051*10^{-8}$ W/[m^2-K^4]
σ_c	=	critical normal stress, MPa
σ_y	=	normal yield stress, MPa
τ_y	=	shear yield stress, MPa

II. Introduction

In fulfillment of the Accreditation Board for Engineering and Technology (ABET) accreditation requirements for the Bachelor's of Science Degree in Aerospace Engineering - Astronautics at Arizona State University, a conceptual "Capstone" mission was proposed to develop an unmanned solar-electric-propulsion (SEP) space cargo ship meant to ferry payloads from Low Earth Orbit (LEO) to a Distant Retrograde Orbit around the Moon. This review is submitted as documentation and justification of the design decisions made throughout the senior capstone

project regarding mission architectures, requirements, and subsystems. The mission is designed around the following prompt:

"NASA is developing the evolvable mars campaign (EMC) and plans to use a Lunar Distant Retrograde Orbit (LDRO) to stage space systems for various missions ranging from lunar excursions, asteroid rendezvous, and Mars exploration by humans. Recent advances in electric ion propulsion and large arrays for solar power generation allow space systems to be transferred from one location to another at lower cost than chemical or nuclear propulsion. The development of 200kW tugs using SEP between LEO and LDRO and larger SEP systems with 500kW for Mars exploration are needed. Teams will design and analyze potential concepts and systems to provide the ability to achieve a 200kW SEP tug for transferring payloads between LEO to LDRO and LDRO to LEO. The space components are to be launched on one (or more) available launch vehicle(s).. Aggregation and assembly of the SEP vehicle components will take place in LEO."

The Evolvable Mars Campaign is NASA's current initiative to facilitate human exploration of the red planet and its neighbors over the next few decades. The initiative includes plans to construct the Deep Space Gateway, a station similar to the International Space Station placed in a Distant Retrograde Orbit around the Moon. This is a highly stable orbit, and is conducive to the staging operations required by manned lunar excursions and deep space missions to the likes of Mars and Ceres. As such, a space vehicle dedicated to transporting cargo from LEO to LDRO and back is needed, both to enable the construction of the Deep Space Gateway, and to service the logistical needs of the Gateway throughout its operational lifetime. The proposed vehicle is dubbed Solar-Propulsive Interplanetary Re-supplier, or SPrIntR. Required concepts also include a scaled up version with a service destination of a Mars orbit rather than LDRO as manned Mars excursions begin to take place.

Over the past thirty years solar cell technology has dramatically advanced, with some cell efficiencies approaching 40%, allowing array specific powers as high as 150 W/kg at their beginning of life in Earth space. This has in turn increased the attractiveness of electric propulsion (EP) systems for all types of space missions, especially with advances in EP technology allowing some thrusters to reach power efficiencies upwards of 70%. With large spacecraft power levels on the order of 10^5 Watts now attainable, large payloads that are already in orbit can be transported much more efficiently with EP, saving tens of thousands of kilograms of propellant, albeit at a slower pace. While this slower pace may not be an attractive solution to the transfer of humans through space, it presents a great opportunity for unmanned craft to more cheaply transport vital cargo to human explorers across the solar system.

A. Literature Review

A space cargo mission of this scale has yet to be attempted by any space program to date. Cargo space modules have been developed by several private companies and national space programs for the purpose of resupplying the International Space Station, but these modules are transported via Earth launch systems and have relatively small payload capacities usually less than 7,000 kilograms. This leaves a relatively small amount of prior art or literature to draw from concerning the specific nature of the problem, and allowed architecture decisions to develop organically within the team. While there is no "tangible" prior art regarding SEP space cargo tugs, this design problem was given as a NASA Big Ideas competition prompt in previous years, allowing the team to do some research and gain insight on previous teams' design proposals. The SPrIntR team's proposal goes further in depth than any previous SEP space tug proposals to date, with more tangible subsystem design and extensive modeling and simulation.

While its mission was purely scientific, information from the development of NASA's Dawn Spacecraft was especially useful for the team in the development of SPrIntR's propulsion and structure subsystems, as Dawn is the largest and most technologically advanced interplanetary SEP spacecraft launched to date.

Additionally, specific information was acquired to ensure the safety of SPrIntR and its payload. The two main dangers the SPrIntR faced was the MMOD environment and docking operations. This resulted in the use of NASA's MMOD protection design hand book and the international docking requirements handbook. This review allowed for a design solution to take place while meeting the requirements set by the mandate and the geometry of SPrIntR. The thermal design for SPrIntR was drawn heavily from Gilmore's Spacecraft Thermal Control Handbook: Volume I: Fundamental Technologies to determine material properties and how to construct a thermal model of a spacecraft.

More generalized spacecraft subsystem design information was garnered from Wertz, Everett, and Puscell's Space Mission Engineering: The New SMAD 1st Ed (SME) [1], as well as the information presented in the present

senior design class. Papers sourced from NASA's Technical Reports Server provided extensive knowledge about electric propulsion and propellant management systems and their implementations. These sources, along with online publications and articles, served as primary and secondary references throughout the design process, and are cited throughout this text. Commercially available information on launch vehicles, spacecraft components, and prior spacecraft designs were also researched and referenced when necessary.

B. Architecture Space

1. Overview

Initial development activities consisted of drafting and evaluating several candidate overall mission architectures. Each team member developed a candidate architecture that fulfilled top-level requirements to be evaluated by the team as whole. This was decided as the best method because the mission mandate gave a fairly specific concept of operations, necessitating overlap in candidate architectures. This allowed team members to collaborate on candidate architecture development while contributing personal perspective and flair. In the end, four main candidate architectures were developed and evaluated by the team. With spacecraft operating power set by the mandate, payload mass, structural mass, and mission time were left as open mission parameters for each architecture, and the main design drivers and differences between each architecture mainly consisted of the following:

- Payload placement and capture
- Solar array configuration
- Electric thruster choice and array size
- Resultant estimated upper-end dry mass (no payload and no propellant)

Due to its specific mission and high power level, the propulsion subsystem of SPrIntR is arguably one of its largest design drivers. The mission mandate, however, gave too little constraints to calculate an optimum specific impulse or mass flow rate using Stuhlinger's [2] optimization methods. This necessitated an approach consisting of optimizing the mission for a specific thruster choice rather than vice-versa, and therefore thruster determination was incorporated into candidate architecture development. Thruster array size was determined by estimating a preliminary power fraction dedicated purely to the propulsion subsystem out of the total 200 kilowatts, and dividing that by the maximum power draw of the chosen thruster. In researching literature and prior design proposals, it was decided that 150 kilowatts dedicated to propulsion is a reasonable fraction for preliminary computations. Dry mass was estimated using the architecture's dimensions and material properties of space-grade aluminum, as well as the specific power of the selected solar array technology.

To compare and evaluate the candidate architectures, several key metrics were developed based on the effects the above differences have on the performance of the spacecraft, specifically from a cargo transport use-case perspective. This allowed the team to distill the "good" aspects of each candidate into a final system architecture. These metrics and trade studies are discussed below.

2. Candidate Architectures

a. Architecture A

Candidate Architecture A consisted of a cylindrical main bus and symmetric rigid-panel solar arrays. The payload docking interface was located on the face of the cylinder opposite to the thruster array. This array contained six 25 kilowatt JPL Nexis thrusters. Its dry mass was estimated to be 5200 kilograms.

b. Architecture B

Candidate Architecture B consisted of a large, half-cylinder main bus with body mounted solar arrays along the face of the half-cylinder. The underside of the half-cylinder acted as the payload bay, and an attached payload module would complete the cylinder. The thruster array was placed on the rear face of the cylinder and consisted of thirty-three 4.5 kilowatt Fakel EDB SPT-140 hall thrusters. This architecture's dry mass was estimated to be about 12,000 kilograms.

c. Architecture C

Candidate Architecture C consisted of a modular, truss-based bus with multiple symmetric rigid-panel solar arrays. The payload and propulsion modules attached to a joint at the center of the bus. The propulsion module consisted of five 30 kilowatt X3 Nested Hall Thrusters. This architecture's dry mass was estimated to be 8,000 kilograms.

d.   Architecture D

Candidate Architecture D consisted of a rectangular main bus with two symmetric rigid-panel solar arrays and a hollow underbelly for receiving the payload module. The thruster array consisted of twenty-one 7 kilowatt NASA's Evolutionary Xenon Gridded Ion Thrusters (NEXT). This architecture's dry mass was estimated at 7000 kilograms.

3.   Down-Selection
a.   Metric Overview

After the candidate architectures outlined in Section II.B.2 were synthesized, six key metrics were developed by the team to evaluate the "goodness" of each system architecture from a cargo transport perspective. These metrics are discussed in the paragraphs below and are as follows:

- Dry Mass
- Ballistic Coefficient
- Array Fundamental Frequency
- Thruster Choice Life Expectancy
- Optimized Transportation Rate
- Required Propellant Mass for Optimized Payload (1 Cycle)

b.   Dry Mass

As mentioned above, dry mass was estimated using the architecture's dimensions and material properties of space-grade aluminum, as well as the specific power of the selected solar array technology. Dry mass was selected as a metric because it has a direct impact on the amount of payload the craft can transport for a given propellant mass.

c.   Ballistic Coefficient

A spacecraft's ballistic coefficient is proportional to its wetted area, and therefore architectures with larger wetted areas were assumed to have larger ballistic coefficients. Ballistic coefficient was chosen as a metric because SPrIntR will spend a significant amount of time in LEO as it performs payload and maintenance operations, as well as the beginning of the transfer spiral to LDRO itself. Atmospheric drag is still present in LEO, and with the low thrust given by electric propulsion, a higher ballistic coefficient leads to a higher minimum orbit altitude that needs to be maintained by the spacecraft. This higher minimum altitude would likely increase costs associated with staging the payload in LEO for pickup by the SPrIntR.

d.   Array Fundamental Frequency

The solar array's fundamental mode flexible body vibration frequency can be approximated as inversely proportional to the square root of the cube of the array's arm length measured from its attachment point. This characteristic is mandated by the prompt to be 0.05 Hz or greater, and was therefore added as a metric to evaluate candidates. Architectures with longer solar array arms were assumed to have lower fundamental frequencies.

e.   Thruster Life Expectancy

The life expectancy of electric thrusters are determined experimentally by the manufacturers, and were mostly determined through online research and from information in SME [1]. Incorporating thruster life expectancy as a metric was an obvious decision, as increased maintenance intervals are highly undesirable and expensive for in-orbit spacecraft.

f.   Transportation Rate & Propellant Mass

Transportation rate for a mission cycle was derived as a metric to be able to characterize the effectiveness of the architecture in terms of its specific mission: cargo transport. It was defined as

$$\frac{Payload\ Mass}{Outbound\ Transfer\ Time} \tag{1}$$

and has units of kg/day. These parameters are interdependent, and a MATLAB tool was built to numerically optimize each architecture's transportation rate for their determined structural mass and thruster array characteristics.

The tool takes arguments of spacecraft dry mass (without payload or propellant), estimated Delta-V for a one-way transit, thruster specific impulse, propulsion system efficiency, and total power available to the propulsion system. Most of these equations are adapted from Jahn [3]. The total mass flow rate of the thruster array is calculated using

$$\dot{m} = \frac{2\eta P_{in}}{\left(9.81 I_{sp}\right)^2}$$

(2)

where η is the efficiency of the propulsion system, P_{in} is the power in Watts available to the propulsion system, and I_{sp} is the specific impulse of the thruster in seconds. The total thrust is calculated with

$$T = \dot{m} I_{sp} 9.81$$

(3)

The propellant required for the return trip without the payload is calculated with the ideal rocket equation,

$$M_{pback} = e^{\frac{\Delta V}{9.81 I_{sp}}} M_s - M_s$$

(4)

where M_s is the spacecraft's dry mass in kg, and ΔV is the estimated Delta-V in m/s required for a one-way transit between destinations. A vector of possible payload masses (M_l) is generated and used in the ideal rocket equation to calculate the total propellant required to transport each prospective payload mass.

$$M_p = e^{\frac{\Delta V}{9.81 I_{sp}}} \left(M_s + M_l + M_{pback}\right) - \left(M_s + M_l + M_{pback}\right)$$

(5)

The time required to transport the payload to the desired orbit is then calculated by dividing the propellant masses by the mass flow rate:

$$\Delta t = \frac{M_p}{\dot{m}}$$

(6)

And the transportation rate is then defined as the payload mass divided by the time required to transport the payload:

$$\Psi = \frac{M_l}{\Delta t}$$

(7)

Finally, the payload mass is optimized by maximizing the function

$$f(M_l) = \frac{\Psi}{M_p}$$

(8)

This maximization represents a clear optimum because as the payload mass increases, the transportation rate increases asymptotically while the required propellant mass increases linearly. This maximization shows the point at which the higher transportation rate gained by increasing the payload mass is outpaced by the increase of required propellant mass. In other words, *this shows the point where increasing the payload mass is no longer economically desirable for the overall mission due to the cost of propellant*.

4. Current Incarnation
    Some revisions and additions to the chosen system architecture have been made as the design matured and new requirements and constraints were identified. First, the concept of underbelly payload docking was determined to be logistically undesirable due to uncertainties in cargo density and the added difficulties associated with payload rendezvous. Research was unable to determine a valid and constant cargo density to plan the dimensions of the craft

6

around, and therefore a docking interface akin to candidate architecture A's was selected. Next, further research into deployable solar arrays showed that Orbital ATK's circular MegaFlex™ arrays give much better frequency and mass characteristics than rigid-panel arrays for large power applications, and were therefore selected for the system architecture. This choice is discussed further in the section describing the power subsystem.

The current system architecture consists of a three meter by three meter by six meter rectangular main bus with symmetric circular solar arrays that are approximately twenty-one meters in diameter. The payload interface is located on the forward face of the craft, opposite of the propulsion module, which consists of the twenty-five NEXT thrusters. The thruster deck was increased from the original twenty-one because of identified power requirements of other subsystems being lower than originally estimated. The core of the spacecraft is a carbon composite cylinder that runs the length of the craft and encapsulates a two meter diameter spherical Xenon tank. Encapsulating the cylinder are six magnesium alloy plates with titanium reinforcement sections where the solar arrays attach to the walls. This allows a sizeable amount of internal volume to be used by subsystem components. The current dry mass estimate of the craft stands at about 10,000 kg. With this current configuration SPrIntR will have a maximum cycle payload mass of 12,000 kilograms and a total cycle time of around 16 months, with a required propellant mass of about 6,000 kg per cycle, where one mission cycle is defined as the transfer from LEO to LDRO and back. This maximum payload mass can be split between destinations in a mission cycle. For example, the client can request that the SPrIntR transport 6,000 kg of cargo from LEO to the moon and transport another 6,000 kg from the moon back to LEO, or they can request the full 12,000 kg of cargo be transported to the moon from LEO, but in this case SPrIntR must make the return transit back to LEO without a payload to refuel.

For the extensible Mars phase of the mission, the original architecture discussed above is scaled up in size to support the addition of larger solar arrays, a larger thruster deck, and a larger propellant tank. The Mars configuration SPrIntR will have a maximum cycle payload mass of 24,000 kilograms and a total cycle time of about 2.7 years, with a required propellant mass of about 31,000 kg per cycle.
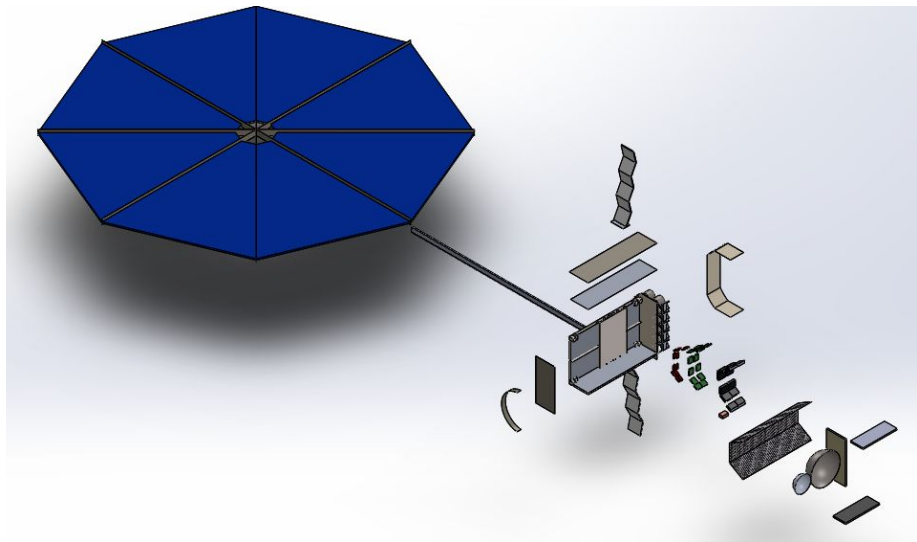

Fig. 1 Exploded Section View of SPrIntR.

C. Subsystems Overview
1. Power
a. Flow Down From Top-Level Requirements
- The craft's solar array area shall produce 200 kW at beginning of life.
    - → This dictates the planar area of the solar arrays.
- Design concepts shall be extensible to 500kW for deep space missions.
    - → This dictates the Mars mission phase solar array area.
- Module joints and arrays must sustain loads up to 0.4 g's of acceleration.
    - → This flows down to the design and construction of the solar arrays themselves.
- The fundamental mode flexible body vibration frequency shall be 0.05 Hz or higher.

7

- ○ → This flows down to the design and construction of the solar arrays themselves.
- ● The spacecraft shall be capable of safely transporting cargo between LEO and LDRO
  - ○ → Due to eclipses associated with EP spiral-out orbit transfers, the power subsystem shall be capable of maintaining at least the minimum spacecraft operating power required for system health during eclipses.

b.   Selected Architecture

The full design and interfaces of the power subsystem can be seen in Fig. 2. Each component and design consideration is discussed in the following sections.

i.   Power Generation

The mission mandate gave that the SPrIntR must be solar powered, and that these solar arrays must produce 200 kW of power at their BOL (beginning of life) for the Lunar phase of the mission, and 500 kW of power at BOL for the Mars mission phase. This gives constant values for which the size of the arrays can be computed for each mission phase. Orbital ATK's MegaFlex arrays were chosen for their flight heritage, high strength, high deployed stiffness, and compact storage volume. The current generation of these arrays are 30% efficient Triple-Junction Gallium-Arsenide cells, giving a specific power of 150 W/kg, and a planar energy density of 288 W/m^2 [4]. The SPrIntR will have two MegaFlex wings, making each wing 666.67 kg and 21 m in diameter for the Lunar mission phase, and 1666.67 kg and 33.25 m in diameter for the Mars mission phase.

ii.   Power Storage

The selected power storage subsystem architecture the LDRO SPrIntR consists of two 250 kW-hr Lithium-Ion secondary batteries, each with a depth of discharge of 30%. Two batteries have been selected for system redundancy and increased spacecraft lifetime. From SME[1], the average specific energy of Li-Ion batteries is about 200 kW-hr/kg, putting the total mass of the batteries at 2,500 kilograms for the Lunar phase. For the Mars mission phase, two 30 kW-hr batteries with a total mass of 300 kg have been chosen. The reasoning behind this much smaller battery size for the Mars phase and the power scheduling issues and discharge levels associated with solar eclipses throughout the spacecraft's transfer are discussed below.

iii.   Power Regulation & Control

Main Bus Power Control

SPrIntR uses a Maximum Power Point Tracking (MPPT) scheme to regulate power to the main power bus. MPPT uses a DC-DC converter in series with the arrays that dynamically changes the resistive load on the arrays and extracts the maximum possible power from them in all environmental and load conditions.

Power Distribution

SPrIntR distributes its power using a decentralized scheme. A decentralized power distribution scheme consists of an unregulated main power bus with tailored POL (Point of Load) converters placed at each spacecraft load as necessary.
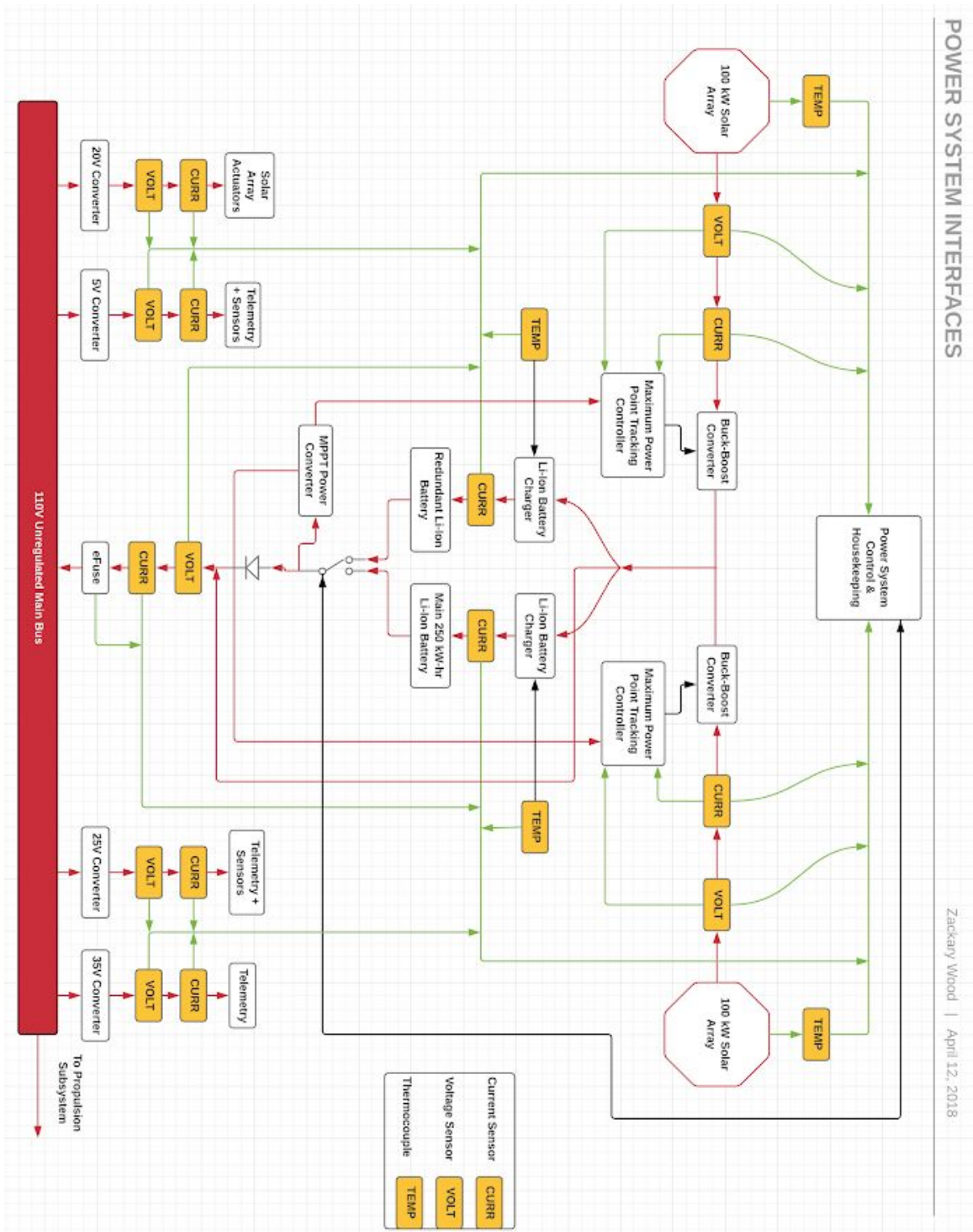
Fig. 2 Power Subsystem Design.

9

Battery Charging Scheme

SPrIntR's batteries are charged individually rather than in parallel.

c.   Selection Criteria & Reasoning

i.   Power Generation

Solar power generation was mandated by the mission prompt, leaving only the array style and geometric configuration to choose. Rigid-panel arrays were originally selected for the spacecraft in two different configurations, but research showed that Orbital ATK's Megaflex™ solar arrays are a third of the mass, 3 to 8 times stiffer, and take up three quarters less volume while stowed compared to standard rigid-panel arrays [4]. Along with the momentum analysis discussed in Section III.C.4, all of these characteristics correspond favorably to top-level requirements and the identified metrics, and so the MegaFlex arrays were chosen.

ii.   Power Storage

Battery Size

Over the course of its lifetime, SPrIntR will periodically experience solar eclipses throughout its spiral transfer orbit to the Moon and Mars. This presents the team with two options: simply operate at full power while the craft is in the sun and shut down all nonessential subsystems while in eclipse or design a power storage system that allows the craft to continue thrusting throughout eclipse. An analysis showed that thrusting at full power in the sun and not thrusting while in eclipse ran the risk of highly ellipticizing the craft's transfer orbit. While this option saves considerable mass due to the absence of large batteries, this elliptical transfer orbit seemed to complicate the required injection into LDRO, especially without access to high-fidelity trajectory plotting software. It was thus decided that the lower complexity and better predictability of a circular transfer orbit outweighed the undesirable effects of the additional battery mass required, and the high-power storage system was designed.

The analysis performed in section IV.B showed that the great majority (>80%) of eclipses that SPrIntR will encounter happen in LEO, usually from altitudes of 400 km to 19,000 km, and will last 35-40 minutes. Less likely eclipses are possible when the craft happens to be at altitudes of 22,000 km to 41,000 km during the spring or fall equinoxes, and these can last up to 65 minutes. In the highly unlikely event of SPrIntR being in or near Lunar orbit during a total lunar eclipse, the craft could experience an eclipse that lasts up to 3.5 hours, but mission operations will preclude this possibility. With the majority of eclipses happening in LEO, this phase becomes the power storage subsystem design driver.

As stated above, lithium-ion batteries were chosen for their high energy density and high cycle life at 30% DOD (depth of discharge). The batteries were sized by building a power balance in Microsoft Excel that models the first day of the transfer orbit beginning in LEO at an altitude of 400 km, with an eclipse time of 35 minutes. This frequency of eclipses in LEO requires a power schedule that allows the batteries to be fully charged in the time that the craft is in the sun without overcharging, while also not allowing the battery's state of charge to drop below the specified DOD percentage. To achieve the goal of operating at the same power in both sunlight and eclipse so as not to ellipticize the transfer orbit, the following power balance was constructed for the Lunar mission phase using a spacecraft operating power of 122.5 kW in and out of eclipse with a battery capacity of 250 kW-hr.
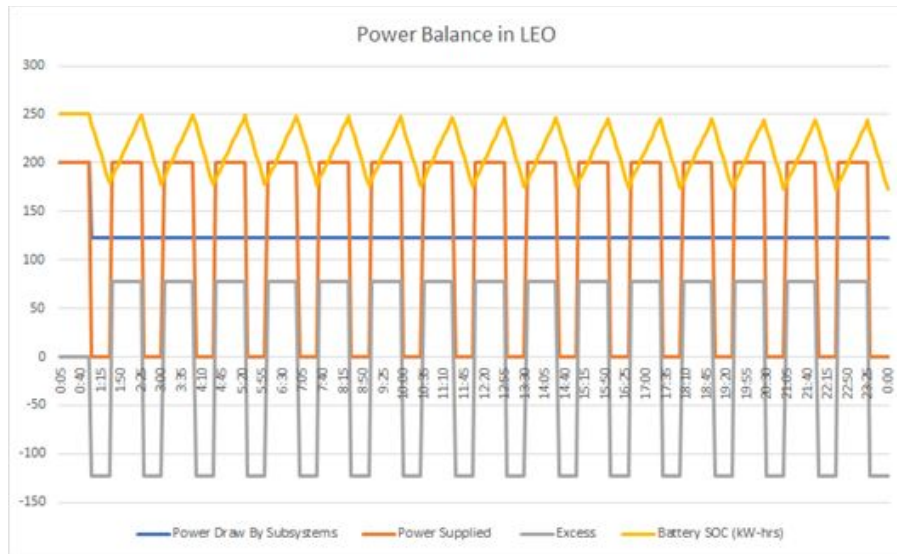
Fig. 3   Lunar Mission Phase Power Balance. *The yellow line is the battery state of charge in kilowatt-hours, the blue line is the constant power draw of spacecraft subsystems, orange is the power supplied by the solar arrays, and gray is the excess power being funneled to the batteries.*

During the less frequent ~60-minute eclipses, the battery DOD can be increased to 50% with negligible effects on battery life to allow SPrIntR to operate at ~125 kW during eclipse.

For the Mars mission phase the same design philosophy was initially followed, however, after revisitation it was realized that without the need to capture a Lunar orbit, the complications that arose from the ellipticization of the transfer orbit from the lack of large batteries did not hold for a transfer orbit to Mars. Having an elliptical burn-out from Earth can actually increase the efficiency of the burn, as long as the transfer is initiated at a time that ensures the final apogee (or where SPrIntR leaves Earth's sphere of influence) of the transfer will occur on the Mars side of Earth. For this reason, smaller 30 kW-hr batteries have been selected that will allow SPrIntR to keep critical systems alive during eclipse, while powering down its thruster bank. The eclipse frequency discussed above is still the same, with >80% of eclipses occurring in LEO. The probability of an eclipse becomes insignificant after SPrIntR leaves Earth's sphere of influence. A power schedule for LEO similar to that above has been constructed for the Mars mission phase, using a dayside operating power of 485 kW and a nightside operating power of 22 kW:
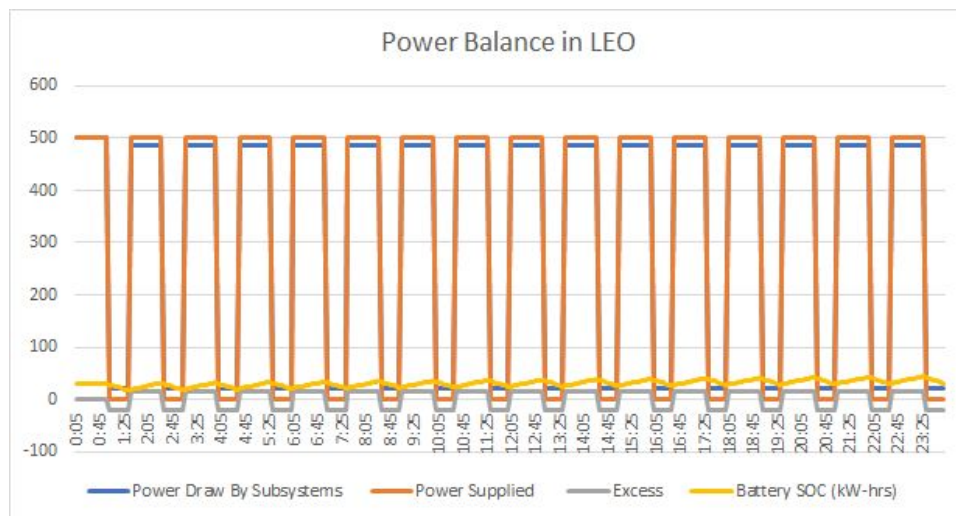

Fig. 4   Mars Mission Phase LEO Power Schedule.

11

Note that with these smaller batteries, some shunting may be necessary at times to avoid battery overcharge.

Battery Chemistry

Technological strides in Lithium-Ion battery technology have made them an attractive choice for space applications due to their high energy density and cycle life. SME [1] puts current Li-Ion average energy density equal to 200 W-hr/kg, and gives the following cycle life vs. depth of discharge curve.
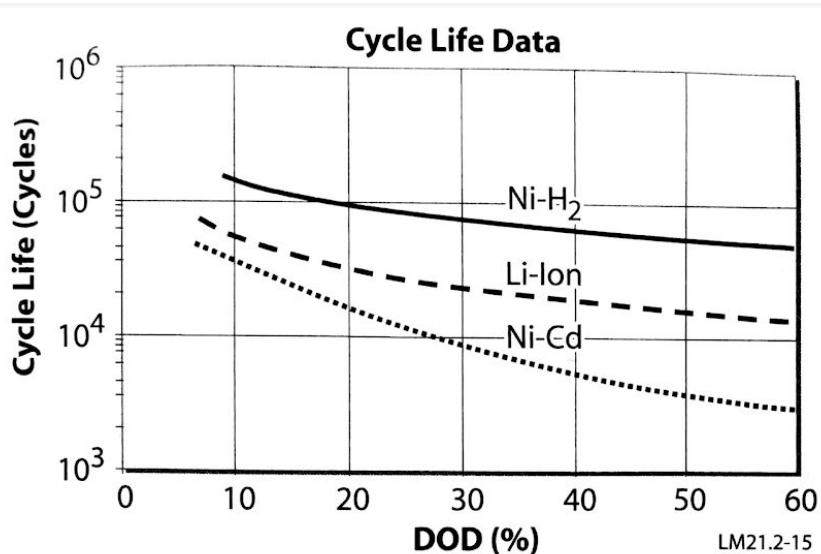

Fig. 5 Cycle Life vs. DOD for Different Battery Chemistries [1].

Because of its high energy density and mid-range cycle life, Li-Ion batteries were chosen for SPrIntR. With a 30% DOD, Li-Ion has a cycle life of ~15000 cycles, which, even if the craft were to only operate in LEO at full power, would give a lifetime of more than two years. This should give the battery a lifetime of greater than ten years for standard operating conditions.

iii. Power Regulation & Control
Main Bus Power Control

With regards to the control of the main power bus, SME [1] gives two commonly used options: DET (Direct-Energy-Transfer) and PPT (Peak-Power-Tracking). DET uses shunt regulators in parallel with the solar arrays to dissipate any excess power not being used by the spacecraft loads and maintain the bus voltage at a predetermined level, often below that of the solar arrays' maximum operating voltage. DET is very efficient and less complex than PPT, but it does not allow the spacecraft to extract the full power of the solar arrays at all times. PPT uses a DC-DC converter in series with the arrays that dynamically changes the resistive load on the arrays and extracts the maximum possible power from them in all environmental and load conditions. PPT systems are less efficient and more complex than DET systems, but because of the nature of SPrIntR's mission and the fact that any excess power not used by the craft's secondary loads will be funneled directly to the propulsion system, a PPT scheme will ensure the shortest transfer times and is the logical choice for the Power Regulation & Control Architecture.

Power Distribution

Power distribution schemes can be centralized or decentralized. Centralized schemes regulate the power to all spacecraft loads within the main power bus, while a decentralized scheme consists of an unregulated main power bus with tailored POL (Point of Load) converters placed at each spacecraft load as necessary. According to SME [1],

12

both high-power spacecraft and those that utilize PPT benefit in efficiency with an unregulated, decentralized power distribution system, and as such, SPrIntR's power distribution scheme will be unregulated and decentralized.

Battery Charging Scheme

Batteries can be charged in parallel with the solar arrays or individually. Parallel charging is simple but causes batteries to degrade faster because they may not all receive the same current during charging. SPrIntR's lifetime is estimated to be greater than 10 years, and as such, individual battery charging will be used to prolong the life of SPrIntR's batteries.

2. Propulsion
a. Flow Down From Top-Level Requirements
- The spacecraft shall be capable of safely transporting cargo between LEO and LDRO in its first complete incarnation, and transport cargo between LEO and Mars Orbit in its second incarnation.
    - → SPrIntR requires an electric propulsion system that is able to produce the delta-V's required to make a cycle between LEO and LDRO (14 km/s), and LEO and Mars Orbit (~32 km/s).
- The craft's solar array area shall produce 200 kW at beginning of life, and design concepts shall be extensible to 500kW for deep space missions.
    - → SPrIntR's propulsion system's maximum power level shall not exceed 200 kW in the first incarnation, and 500 kW in the second.

b. Selected Architecture

The following diagram, Fig. 5, shows the full design and interfaces of the propulsion subsystem. All gas pressures and feed line diameters are denoted. Each component and design consideration is discussed in the following sections.
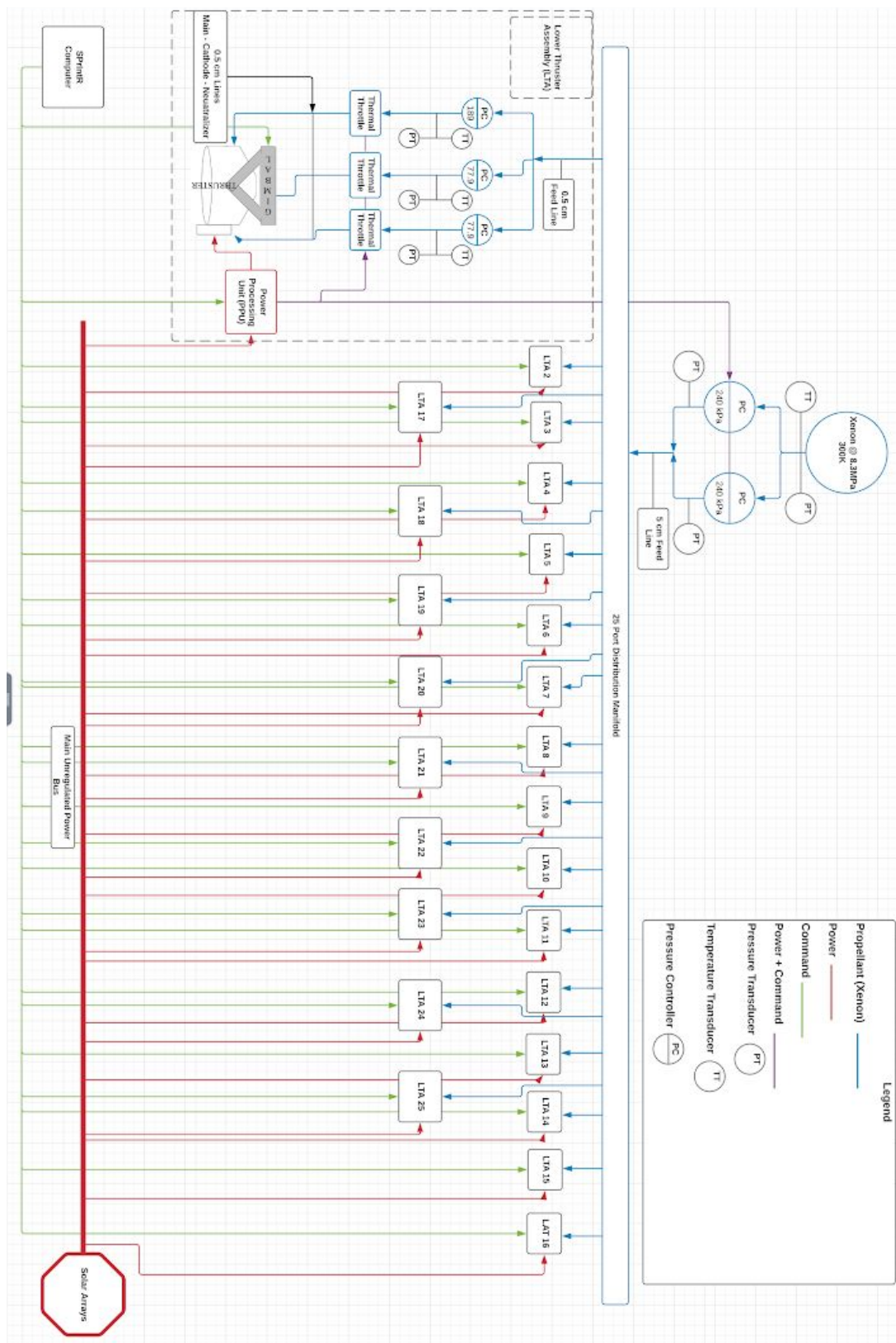
Fig. 6   Propulsion Subsystem Design. Note that the LTA is expanded in the dotted lines for more compact viewing.

i. Primary Propulsion

In the previous semester, the SPrIntR team selected the NEXT (NASA's Evolutionary Xenon Thruster) Gridded Ion Thruster as the primary propulsion engine for the spacecraft. NEXT was selected for its flight heritage, high efficiency (thruster: 72%, system: 67%), high specific impulse (Isp = 4200s), and long lifetime (>55,000 hours) [5]. The preliminary design for the Lunar mission phase called for a thruster deck consisting of 21 thrusters. This was determined using an initial assumption of 150 kW being the maximum power ever available for the propulsion subsystem (a single thruster's maximum power consumption is about 7.2 kW). With the current semester's updated power consumption data from the other subsystem owners, this maximum power level has been amended to 180 kW. This gives a thruster deck consisting of 25 thrusters for the Lunar mission phase, with a total maximum thrust of 5.9 N. This high thruster count allows for a very high level of system redundancy and ensures that any excess spacecraft power can be utilized without detriment to spacecraft systems. Following the same vein, for the 500 kW Mars mission phase, the maximum propulsion subsystem power level has been estimated to be 470 kW, as the power consumption levels for other subsystems do not vary significantly between mission phases. This gives a thruster deck consisting of 65 thrusters for the Mars mission phase, with a total maximum thrust of 15.34 N.

Each full thruster string has a mass of 57 kg. This number includes the thruster's gimbal, PPU (Power Processing Unit), and the PMS (Propellant Management System) components necessary for one thruster. This makes the thruster deck masses equal to 1425 kg and 3705 kg for the Lunar and Mars mission phases, respectively.

The thrusters and their gimbals will be arranged uniformly along the rear face of the spacecraft body. The gimbals have a two-axis range of motion: ±19°, ±17°.

ii. Propellant Management System

The NEXT system's propellant management system consists of three parts: A high-pressure spherical titanium propellant tank containing super-critical Xenon, an HPA (High-Pressure-Assembly) that regulates the supercritical Xenon down to a pressure of 240 kPa and distributes the flow to all of the thruster strings, and an LPA (Low-Pressure-Assembly) that further regulates and separates the flow into the lines for the thruster chamber, cathode, and neutralizer. One HPA can provide flow to multiple thrusters, while each thruster needs their own LPA. One HPA is approximately 5 kg, while one LPA is 3.1 kg.

The propellant tank is made of Ti-6Al-4V (Grade 5) Annealed Titanium, a common space-rated titanium alloy. The Lunar mission phase requires 6000 kg of Xenon propellant per cycle, and is calculated using the payload optimization tool discussed previously. This calculation is also discussed in the payload subsystem section. With this propellant mass, the propellant tank must have an inner radius of 1.02 meters and a wall thickness of 5.3 millimeters. With these dimensions, the mass of the tank will be 306 kg. The Mars mission phase requires 31,000 kg of Xenon per cycle, giving an inner radius of 1.76 m, a wall thickness of 9 mm, and a mass of 1583 kg.

The HPA regulates the flow using a PFCV (Proportional Fluid Control Valve) that uses a pressure transducer for feedback and is controlled by one of the NEXT PPU's. It includes a redundant PFCV and transducer in case of component failure. After the flow pressure is reduced, the HPA uses a distribution manifold to direct the flow to each LPA. For the Lunar mission phase, a 25-port distribution manifold is required, while the Mars phase manifold requires 65 ports. The LPA uses three PFCV's to regulate each branches' flow into three thermal throttles. The PFCV's again have pressure transducers for feedback, and both them and the thermal throttles are controlled by that branch's PPU.

To enable LEO refueling after each mission cycle, the propellant tank will have a valve on the forward side, opposite to the HPA. This valve will be connected to a feed line that runs to a refueling port in the center of the craft's docking mechanism. To refuel, SPrIntR will perform a standard docking rendezvous with a refueling craft, similar in operation to that of a standard payload. Once SPrIntR is docked with the refueling vehicle and a secure connection has been made to the refueling port, valves will open, allowing Xenon to flow into SPrIntR's propellant tank until pressure equilibrium. After equilibrium, the refueling vehicle can use a simple hydraulic piston

mechanism to force the remaining Xenon into SPrIntR's propellant. The same operation will happen for the propellant tank that supplies SPrInR's attitude control system.

c. Selection Criteria & Reasoning

i. Primary Propulsion

As discussed in Section 1.3, the mission mandate was largely open ended, and gave too little constraints to calculate an optimum specific impulse or mass flow rate using Stuhlinger's [2] optimization methods. This necessitated an approach consisting of optimizing the mission for a specific thruster choice rather than vice-versa, and therefore thruster determination was incorporated into candidate architecture development. There were four main trades associated with the preliminary thruster choice:

- Specific Impulse
- Power Efficiency
- Heritage
- Life Expectancy

Heritage was a large driver in each candidate architecture's EP thruster choice. There are many experimental and theoretical EP thrusters that have been proposed, and some of these have some seemingly "too good to be true" performance estimates. The team decided it is best to solve this mission prompt from the standpoint of existing technology, and therefore only attainable and flight-tested hardware was considered. Life expectancy was incorporated into the architecture selection metrics, while specific impulse and power efficiency played significant roles in the transportation rate trade space examined in Section II.C.3. NEXT was selected for its flight heritage, high efficiency (thruster: 72%, system: 67%), high specific impulse (Isp = 4200s), and long lifetime (>55,000 hours).

ii. Propellant Management System

The components of the propellant management system were expanded from the descriptions given by NASA test data for the NEXT system [5]. Each propellant feed line has been sized by ensuring that the flow through the lines remains laminar, which for pipes is generally assumed to mean that the Reynold's number remains less than 2300. The equation below shows the Reynolds number casted in terms of the mass flow rate and viscosity of the gas:

$$Re = \frac{4\dot{m}}{\pi \mu D} \tag{9}$$

Where $\dot{m}$ is the mass flow rate in kg/s, D is the diameter of the line in meters, and μ is the viscosity of the gas in N-s/m². The mass flow rates for each feed line are given by NASA test data [5], while the viscosity of Xenon is mostly dependent on temperature and is available from standard literature tabulation.

The propellant tank is sized by first using Welle's [6] derivation for the optimum storage density of Xenon found by minimizing the tankage fraction as a function of Xenon density for a titanium tank. For Xenon at 300 K, this optimum density occurs at 8.3 MPa. In a thin-walled spherical tank containing a pressurized fluid, the tensile stress in the shell is calculated by

$$S = \frac{Pr}{2t} \tag{10}$$

Where P is the pressure in Pa, r is the inner radius of the tank in meters, and t is the wall thickness in meters. For a safety factor of β, the maximum stress in the wall is limited by

$$S = \frac{\sigma_y}{\beta} \tag{11}$$

Where σ_y is the yield strength of the tank material in Pa. And the radius of the tank is then given by

$$\sqrt[3]{\frac{3M_p}{4\pi \rho_p}} \tag{12}$$

16

Where M_p is the mass of the propellant required for the mission in kg, and ρ_p is the calculated optimum density of Xenon ($\sim$1350 kg/m^3). The total mass of the propellant tank can then be calculated using the dimensions of the tank and the density of the tank material (ρ_t), which in this case is titanium:

$$M_t = 4\pi r^2 t \rho_t$$

(13)

The above equations have been used to create a custom MATLAB tool to expedite calculations, as the overall mass characteristics of the spacecraft change frequently which in turn affect the value of M_p.

3. Structures & Mechanisms

a. Flow Down From Top-Level Requirements
- Maintain fundamental flexible body vibration mode greater than 0.05 Hz.
- Structure must be assembled in LEO within 60 days.
- Module joints and arrays must sustain loads up to 0.4 g's of acceleration.
- Minimize need for extraneous attitude control due to masses offset from center of mass.

b. Selected Architecture

The selected structures & mechanisms architecture uses two solar arrays that would be placed symmetrically around a center body that will house all other subsystem components. The central body has an extended engine plate and flange to house the numerous NEXT ion thrusters. This ensures all preliminary structural and mechanical system requirements are met. Discussion of the body and solar arrays is shown below. A CAD model of SPrIntR's geometrical design can be seen in Fig. 7.
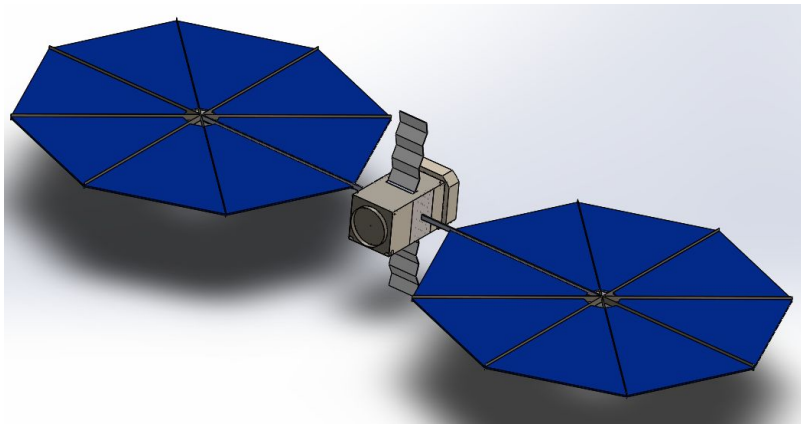

Fig. 7 CAD Model of the Finalized SPrIntR

i. Central Body
Propellant tank

The main constraint in sizing the central body of SPrIntR was the mass of propellant being transported. The propellant needed is Xenon, similar to the DAWN spacecraft. However, the mass of propellant needed for SPrIntR is much greater than that needed for DAWN because of SPrIntR's large mass profile. Utilizing the propellant tank sizing MATLAB tool discussed in Section III.C.2, the required central volume for the tank was found. The total volume needed for the SPrIntR propellant tank was found to be 4.19 cubic meters (ensuring 6000 kg of Xenon could be transported).

Central Cylinder

Realizing that the volume requirement will need to include other subsystem components such as the Xenon feed system, telecommunications systems, ADCS, power storage and management systems, etc., a central cylinder will encompass the propellant tanks and construct the core of SPrIntR. This provides mounting surfaces for subsystem

17

components and aides in transferring forces to the spacecraft body similar to DAWN, this will ensure that SPrIntR can withstand rocket launch conditions. The hexagonal cylinder is made of a graphite composite and has a diameter of 2.54m, a thickness of 1 cm, and a length of 5.03 m. The length of 6 m was a preliminary design choice made in attempts to ensure adequate room in the "annulus" of free space within the central body for subsystems, but was later shortened to 5.03 m to ensure the NEXT thrusters could be attached.

Outer cuboid and payload attachment

The outer cube of SPrIntR will be made from seven AZ-31 magnesium alloy plates and two 6AL-4V titanium support systems with varying dimensions: the front plate will be 3x3m, the top and bottom plates will be 3x5.03m meters and the side plates which surround the truss systems are 3x2m and 3x1m, while the support systems are 3x2m. Each plate will have a thickness of 5.5mm. An universal interface for payload attachment and refueling will be attached to the front of the bus, this interface will encompass a hard docking ring made from AZ-31 magnesium alloy and a soft docking capture mechanism. The decision for attaching the payload to the front of the craft as opposed to stowing it in the underbelly as was previously chosen came from the need to constrain the value of the center body volume while also "lifting" constraints on payload volume. The location of attachment keeps the payload along the thrust vector and in-line with the center of mass of the craft, thus reducing the need for extraneous attitude control due to torques created during normal operating modes.

ii. Solar Array Deployment and Rotation

Orbital's MegaFlex™ solar arrays are equipped with their own deployment modules that have been successfully tested [4]. The solar array module will be attached to the side of the SPrIntR in a horizontal fashion. It will be attached to the SPrIntR when the array is stowed and inside of the rocket fairing. For maneuvering the arrays, two C50 Incremental Rotary Actuator's made by Sierra Nevada Corporation will be used [7]. These actuators can slew at 2.7 deg/sec with a motor providing 45 pulses/sec. This corresponds to 22 microsecond long pulses. The running torque is 112 Nm. Therefore the change in angle that will occur to the spacecraft body from rotating the solar arrays is on the order 5E-7 rad. This is negligible and thus acceptable.

c. Selection Criteria & Reasoning

The chosen architecture is determined by observing several components and characteristics of the structures and mechanisms subsystem.

i. Frequency Characteristics

The requirement for vibrational mode frequency played a large role in determining the allowable geometry of SPrIntR, this requirement ensured that SPrIntR remained stable & efficient when maneuvers were performed. The Orbital ATK MegaFlex™ solar arrays have a predicted stowed fundamental frequency of 30 Hz and a predicted deployed fundamental frequency of 0.27 Hz [4]. Following the preliminary calculations above, a computational analysis was completed using ANSYS. The analysis was conducted by modeling the Megaflex array, strut, and bus wall, then using the known characteristics of the Megaflex component. A disk of the same diameter (21 meters) was created with a thickness which would bring the Mass of the solar array to that of the mass which was computed by the power subsystem. Upon conducting this analysis, the frequency response of the SPrIntR's array was 0.07645 Hz. Thus, the hard requirement that the SPrIntR have a frequency response over 0.05 Hz was completed.

ii. Solar Array Stowage

The requirement to assemble the SPrIntR in 60 days or less encourages a smaller overall spacecraft volume so as to minimize the number of launches that would be required to transport it to LEO. The stowed length of SPrIntR must fit within the launch vehicle fairing that is selected. The stowage length of Orbital's MegaFlex is calculated to have a value of 7m for each 100 kW solar array and 10.66m for each 250 kW solar array. Currently, SPrIntR will be launched on a Delta IV Heavy launch vehicle. The 500 kW design will require one launch using the SLS Block 2B as well.

iii. Subsystem Placement

After the above analyses were computed and performed, a CAD model of SPrIntR was created to visualization how each subsystem was going to interface with the structure of the bus. As can be seen in Fig. 8, the radiator arrays had to be placed on the top and bottom surfaces of the bus to ensure that they would not interact with the solar arrays

18

and dissipated heat would not affect other subsystems. In Figure 8, the thruster array can be seen, the array holds 25 thrusters in a 5x5 square. The back engine plate is larger than the main bus because 25 could not fit on a 3x3 plate due to the gimbels. This slight extension did not change the structural behavior to the buckling analysis. The extended thruster bay has a footprint of 3.65x3.65 meters, the corners of the engine port must be circularized to ensure SPrIntR will fit into the fairing.

In Figure 8, the SPrIntR's internal bay is exposed but the central carbon fiber hexagonal tube is in place. This tube will allow for the subsystems to be attached to the spacecraft. It should be noted that the gray coloring on the top and bottom of the outer bus wall is the MMOD shielding, and the black rectangular cubes on the bottom and top are the batteries. The back half of the SPrIntR is separated by a beige wall. This wall will insulate the sensitive subsystems such as batteries and communications from the power systems such as the PPUs, IPAs, and the HPAs which are attached to the cylinder. This is due to the excessive heat which the power subsystem radiates.
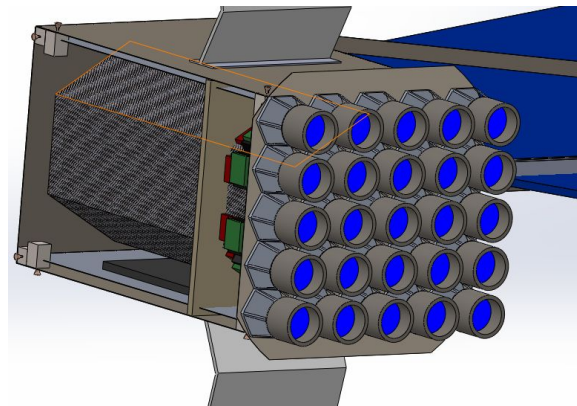

Fig. 8. Thruster Array.

Figure 8 shows the thruster array and their attachment points to the gimbals for each thruster, as well as the circularized corners.

4. Attitude Determination & Control

a. Flow Down From Top-Level Requirements

Because SPrIntR is required to produce 200 kW of power, and therefore has a large solar array area, attitude control is a concern. For smaller spacecraft, it may be enough to simply design the attitude control to counteract disturbance torques in LEO. SPrIntR, however, has additional requirements specific to its low-thrust spiral orbits. In order to continuously raise its orbit, SPrIntR must thrust parallel to the velocity vector (i.e. thrust tangent to its orbital position vector with reference to the Earth). This imposes a slew rate requirement of 2π radians per every orbit. From SPrIntR's mandate, it must be able to sustain loads up to 0.4 g's of acceleration and have a fundamental flexible body vibration mode of 0.05 Hz or higher. The last requirement is to be able to meet the tip-off rates of a payload when rendezvousing. The tip-off rates are taken from known launch vehicle separation characteristics and are discussed in the following sections.

b. Selected Architecture

To fully design the architecture space for this subsystem, several selections needed to be made, such as the optimal solar array configuration for ADCS purposes, the attitude control method, attitude control configuration, operations considerations, and sensor selection.

The optimal solar array configuration was determined to include the Orbital ATK MegaFlex™ solar arrays, such as in Fig. 10. In order to effectively maneuver with such massive solar arrays (about 700 m² in area and 1300 kg in mass) while meeting the slew rate requirement and rejecting disturbance torques, monopropellant Hydrazine thrusters in conjunction with gimbaling of the main propulsion unit was chosen as the desired attitude control method. The spacecraft will utilize a total of 16 Moog-ISP Monarc-22-12 thrusters, as laid out in Fig. 9 below.
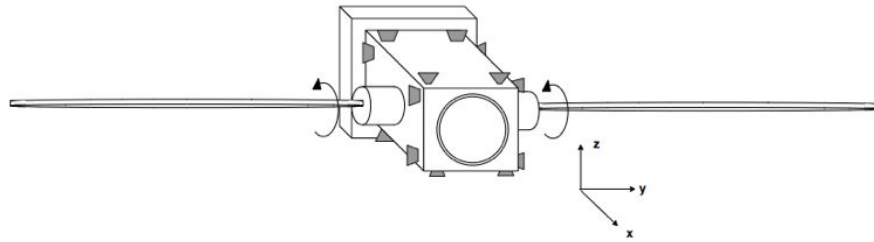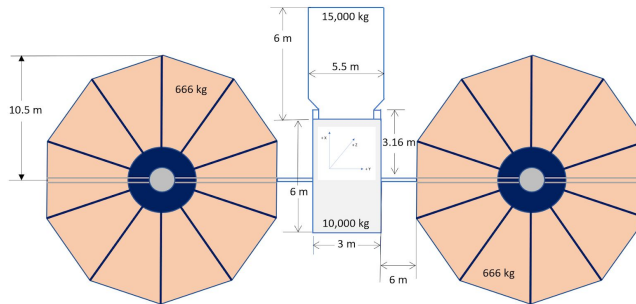
Fig. 9 SPrIntR ACS Thruster Configuration.

Fig. 10 SPrIntR Solar array configuration.

The Monarc-22-12 thrusters will be used to meet the tip-off rate of the payload prior to rendezvous and to provide extra attitude control in emergency situations. The gimbaling of the NEXT array will be used to reject disturbance torques and to keep SPrIntR on its required slew rate.

Lastly, to operate the thrusters, SPrIntR will utilize ground-monitored attitude control while in LEO, but autonomous attitude control throughout the remainder of the mission. To allow the support of autonomous attitude control, SPrIntR will use make use of a sensor suite outlined in the Guidance and Navigation section.

c. Selection Criteria & Reasoning
i. *Attitude Control: Considering Multiple Vehicle Configurations*

To determine the vehicle's maximum momentum requirement, the moments of inertia for each potential solar array configuration needed to be calculated. This analysis was performed on the initial solar array configurations as well as the decided upon MegaFlex™ configuration, and served to help make the final decision on the power generation subsystem architecture as well.

Configuration 1: Solar Array Deployment Along the Pitch Axis

In the first configuration, the solar array deployment, and therefore rotation, is centered on the vehicle's pitch axis. This results in a moment of inertia about the pitch axis (I_y) that is much less than that about the roll or yaw axes (I_x or I_z) at about 50,000 kgm^2. In contrast, I_x and I_z are found to be 1,011,348 kg-m^2 and 1,053,509 kg-m^2 for this configuration, although these numbers were calculated without taking the payload mass into consideration, meaning even the maximum value listed here (I_z) is lower than reality. Using each axis' moment of inertia and the angular momentum equation, with a radial velocity of 0.0087 rad/s roll and 0.026 rad/s pitch and yaw (orbital insertion accuracies of the Delta IV rocket) [8], the maximum angular momentum experienced in each axis during one orbit can be calculated.

However, it is important to note that the launch vehicle selection for this mission has not yet been completed. The use of the Delta IV orbital insertion accuracies are used as a realistic placeholder until data for larger rockets (i.e. Space Launch System (SLS)) becomes available.

For this configuration, the maximum angular momentum is determined to be 26,295 Nms about the yaw axis. Therefore, if the current layout of the solar arrays is maintained, the attitude control system would need to be robust enough to correct forces up to this magnitude.

20

Configuration 2: Solar Array Deployment Along the Roll Axis

Concerns in other subsystems called for a potential repositioning of the solar arrays. For example, the frequency response of the solar arrays when deployed along the pitch axis presents a potential structural issue. Therefore, an alternative vehicle configuration in which the solar array wings are deployed along the roll axis is proposed.

Similar to Configuration 1, the moment of inertia about the axis of solar array deployment (I_x, in this case) is the smallest of the three I values at 524,385 kgm^2. In contrast, I_y and I_z were found to be 723,940 kgm^2 and 753,107 kgm^2, payload mass included. Using the angular momentum equation, with the same radial velocity of 0.0087 rad/s roll and 0.026 rad/s pitch and yaw, the constraining torque is found to be 19,580.78 Nms about the yaw axis.

Configuration 3: Orbital ATK MegaFlex^{TM} Solar Arrays

Similar to Configuration 2, Configuration 3 is a result of needing to address subsystem requirements. While solar array deployment along the roll axis does improve the overall stability and frequency response of the spacecraft compared to Configuration 1, it introduces a new problem: thruster plume impingement. Because SPrIntR's gridded ion thruster array will be positioned on the spacecraft face opposite that of which the payload is attached, allowing solar arrays to deploy along with x-axis significantly increases the likelihood that particles exiting the front of the spacecraft will come into contact with the solar arrays. In an effort to avoid unnecessary solar array contamination, Configuration 3 utilizes Orbital ATK's MegaFlex^{TM} solar arrays.

With approximately 700 square meters in area, the same as that of Configurations 1 and 2, Orbital ATK's product offers a more compact shape with a much smaller mass (a total of approximately 1300 kg [9], as opposed to Configuration 2's 3500 kg total mass). Avoiding the long, cantilever beam-like configuration of the solar arrays in Configurations 1 and 2, as well as decreasing the overall array mass, greatly improves the vehicle's structural state.

Recalculating the moments of inertia in each axis for this configuration results in an I_x of 350,000 kgm^2, and I_y of 430,000 kgm^2, and an I_z of 710,000 kgm^2. These moments of inertia are easily the smallest of the three configurations, leading to an new constraining torque of 18,460 Nms when using the same Delta IV orbital insertion accuracies used for Configurations 1 and 2.

ii.   Attitude Control: Momentum Wheel vs. Thruster Feasibility and Decision

Momentum Wheel Feasibility

For a spacecraft of SPrIntR's size, regardless of the configuration chosen, the best possible case momentum wheel was determined to be Control Moment Gyros (CMGs), roughly the size of those currently on the International Space Station (ISS) [10]. Each CMG has an angular momentum rating of 4760 Nms, which scales up to 19,000 Nms in total momentum storage after considering that four CMGs would be needed (3 for active attitude control, and 1 for redundancy). Although utilizing all four CMGs would be enough to manage Configuration 2, Configurations 1 and 3 have requirements beyond the CMGs' capability.

Further, there are additional complications with using CMGs. While the CMGs (1.29 m x 1.37 m x 1.23 m) can fit within the main body of the spacecraft (3 m x 3 m x 6 m) without altering the current dimensions, using a momentum wheel would require periodic momentum dumping, for which an additional control mode would be necessary. Adding four CMGs to the spacecraft would also require an additional 1,088 kg to SPrIntR's already large mass profile. Further, the design characteristics show that the lifetime of each CMG is roughly 10 years, if they do not experience gimbal lock, as CMGs are known to suffer from periodically, thereby needing a replacement [10]. Overall, there would still exist several concerns with CMGs as a form of attitude control if chosen.

Thruster Selection and Operation

Alternatively, several hydrazine monopropellant thrusters were considered [11]. First, Moog-ISP's Monarc-90LT was inspected, as the thruster offers 90 N of steady state thrust. Considering two couples of these thrusters, with one pair at each end of the main body of the spacecraft (along the roll axis) equidistant from the center of the body, it would take approximately 36 seconds to produce the maximum momentum requirement of the three configurations (19,580 Nms). This, of course, can be improved depending on the placement of the thrusters, as a longer moment arm will result in a higher instantaneous torque, and therefore a larger momentum over time. Moog-ISP also has products offering 22 N, 116 N, and 445 N of thrust, such as the Monarc-22-12, the Monarc-90HT, and the Monarc-445, respectively. The Monarc-445, for example, could produce 19,000 Nms of momentum in just 7 seconds, with the same thruster configuration assumed previously [11]. Because a top-level requirement for this mission is to remain below the 0.4g threshold for structural stability, the 116 N Monarc-90HT is

the best thruster for the chosen solar array configuration, because it is able to produce the maximum momentum requirement of 18,000 Nms in 25 seconds. In addition it provides a large factor of safety, due to it producing 49.6% of the maximum allowable thrust, as per requirements, whereas the Monarc-445 exceeds the 234 N limit by 90%. Additionally, each of these thrusters is less than 2 kg, so adding as many as necessary would barely increase the overall mass profile of the spacecraft. More importantly, with mass flow rates on the order of 0.05 kg/s, a 100 kg hydrazine tank has the potential to support all possible attitude maneuvers over the course of the vehicle's lifetime.

After further calculations and research, a different attitude control method was presented. Using the gimbaling of the NEXT array, the disturbance torques can be exactly countered and the slew rate can be achieved. This leaves the Hydrazine thrusters to function in meeting the tip-off rate of a payload when rendezvousing. With this new architecture, the Hydrazine thrusters can provide significantly less thrust and will require less propellant. These results are shown in the following section and in section IV.C.

iii. Modeling

Several cases are being examined to ensure SPrIntR can meet its attitude control requirements. The first case is a modeling of the disturbance torques that will be encountered. Another case needing to be modeled is the torque required to keep the solar arrays oriented normal to the incoming solar radiation. This is modeled in conjunction with torque required to slew the spacecraft the right amount so as to keep the thrust vector tangent to the orbit at all points in the orbit.

iv. Attitude Control: Thruster Quantity & Placement

The main concern with using thrusters for attitude control is the potential to contaminate the solar arrays. In order to mitigate this, the thrusters will be used only for a brief amount of time when meeting the payload tip-off rate as discussed in the previous section. All additional attitude control can be handled by the gimbaling of the NEXT array, while the Hydrazine thrusters can be used for worst-case scenarios.

v. Attitude Determination: Sensor Selection

For attitude determination purposes, sun sensors, star trackers, an inertial measurement unit, and a relative range sensor will be used. The complete trade study performed to determine the sensor models is shown in section 2.3.5 (Guidance and Navigation). However, with the sensor suite selected, complete 3-axis attitude along with position and velocity data can be retrieved and combined in the on-board computer's estimator (e.g. Kalman Filter) to provide the best state vector estimates.

5. Guidance & Navigation

a. Flow Down from Top-Level Requirements

From the top level requirements, the SPrIntR shall ferry a payload in a low-thrust spiral orbit from LEO to a LDRO. Once in the LDRO, SPrIntR will separate with the payload. After this phase, SPrIntR will return to LEO where it will refuel and rendezvous with another payload for transport. Alternatively, SPrIntR has the capability to separate with a payload at LDRO and then rendezvous with a different payload that can be transported back to LEO. One pivotal requirement is SPrIntR's power production of 200 kW. This requires the solar arrays to maintain an orientation normal to the incoming solar radiation at all points in each orbit. For continuous acceleration in a low thrust orbit, the thrust vector must remain parallel to the velocity vector. This implies a required slew rate of 2π rad every orbit, while keeping the solar arrays normal to the sun.

In addition to the LDRO phase, SPrIntR must be extensible to complete a Mars mission phase where it will travel from LEO to a 5 Sol orbit and back. Due to the communication requirements at such large distances in the Mars mission phase, autonomy will be required at certain phases.

b. Selected Architecture

The architecture for the Guidance and Navigation (GN) subsystem was selected in conjunction with the design for the ADCS. A block diagram of the interaction between the ADCS and GN subsystems can be referenced from [12]. The selected sensor suite will provide complete 3-axis attitude information along with position and velocity readings. The various mission phases encountered by SPrIntR are described in the following subsections.

i.   Components

The GNC components are summarized in Table 1, the selection criteria and reasoning is discussed in the following section.

Table 1. GN Hardware Components with Corresponding Data Output

Sensor	Model	Data Output
Star Sensor	HYDRA-M	3-Axis Attitude
Inertial Measurement Unit	LN-200S	Position, Velocity, Angle Rate
Sun Sensor	MSS-02	Attitude, Sun Vector
Range Sensor	TriDAR	Range and Tracking

c.   Selection Criteria & Reasoning

i.   Navigation Architecture

Selection

SPrIntR will utilize all three of the above stated navigational systems for different mission phases as well as Mars extensibility. The ground based navigational system which is going to be utilized is the deep space network. This network will be used for the Mars extensibility mission during transit and orbit around Mars. This selection was made due to the extreme distance in which the DSN can transmit data, as well as due to its "position accuracy of 150m at a distance of 1 AU" [1]. In addition, the DSN has "four locations spread across earth at 120 degrees apart in latitude…which permits a constant observation of a spacecraft" [1]. SPrIntR will utilize TDRSS when in LEO and in transit to LDRO. TDRSS was selected due to it being a space based system, therefore bypassing atmospheric interference, as well as having a quicker relay period. The TDRSS also has multiple spacecraft in orbit around the Earth, therefore coverage is constantly available. TDRSS can achieve 3σ accuracies of about 50 meters [1]. Autonomous navigation will be utilized during LEO to LDRO transit past GEO as well as when SPrIntR is orbiting in LDRO. This will be utilized due to the noncritical nature of the transit and the orbit within LDRO, SPrIntR should be able to monitor itself and only contact a navigation system if there is a malfunction or an error within its autonomous system. The DSN can be called upon in this case, but it is not optimal because the DSN is designed for spacecraft outside of the Earth's sphere of influence.

ii.   Components

Sensor Selection

The sensor suite is chosen to consist of star trackers, sun sensors, an inertial measurement unit, and a range sensor for payload/rendezvous operations. To choose specific hardware components, a trade study was conducted for each sensor type: inertial, sun, and star. Once the data was gathered, the individual trade studies could begin. The inertial sensors were ranked from most important to least important by power, mass, drift, and size. As can be seen in Table 2, the LN-200S IMU from Northrop Grumman was selected [13]. The sun sensors were ranked from most important to least important by mass, accuracy, size, and power. This trade study, shown in Table 3, resulted in the MSS-02 made by Space Micro for sun sensors [14]. Lastly, the star tracker trade was ranked from most important to least important by accuracy, size, field of view, slew rate, power, and mass. The winner, as can be seen in Table 4, was the HYDRA-M made by Sodern Optronic Space Equipment [15].

23

Table 2. Trade study results for inertial sensor selection. *Note the LN-200S scored the highest.*

	Manufacturer	Northrop	Northrop	ATA
Category	Weight	SIRU-E	LN-200S	IMU
Power, (W)	4	1	3	2
Mass, (kg)	3	1	3	2
Size, (m^3)	1	1	3	2
Drift, (deg/sqrt(hr))	2	1	2	3
	Total Score	10	28	22

Table 3. Trade study results for sun sensor selection. *Note the MSS-01,02 scored the highest.*

	Manufacturer	MOOG	JenaOptronik	Adcole	Space Micro	Optical Energy Te	SSTL
Category	Weight	Fine Sun Sens	Fine Sun Sens	Digital Sur	MSS-01,02	Sun Sensor	DMC Sun Sensor
Power, (W)	1	1	2	3	6	5	4
Mass, (kg)	4	3	2	1	6	5	4
Size, (m^3)	2	4	2	1	6	3	5
Accuracy, (deg)	3	5	6	7	1	4	3
	Total Score	36	32	30	45	43	39

Table 4. Trade study results for star sensor selection. *Note the HYDRA-M scored the highest.*

	Manufacturer	JenaOptronik	JenaOptronik	Sodern	Terma
Category	Weight	ASTRO-15	ASTRO APS	HYDRA-M	HE-5AS
Power, (W)	2	2	1	3	3
Mass, (kg)	1	1	2	3	2
Size, (m^3)	5	1	4	3	2
FOV, (deg)	4	1	2	4	3
Accuracy, (arcsec)	6	1	1	2	3
Slew Rate, (deg/s)	3	1	1	3	2
	Total Score	23	41	61	54

6. Telecommunications

a. Flow Down From Top-Level Requirements

There were two main factors driving the design of the communications systems: (1) the spacecraft shall be capable of transporting cargo between LEO and LDRO. This creates an issue in the form of free space losses at the Moon. Therefore, the antenna gain, and therefore the antenna diameter, will need to compensate for this loss. (2) The spacecraft's solar arrays will need to produce 200 kW at BOL. This highlights the need for the communications system to draw as little power a possible. Based on these two requirements, the antenna size and power draw were optimized such that an overall positive margin was achieved.

b. Selected Architecture

The selected architecture uses Ka-Band to achieve the high data rate for communications in LEO, at the Moon, and at Mars. At distances up to, and including an orbit around, the Moon, the data rate will be fixed at 1 Mbps for uplink and 5 Mbps for downlink. This will be accomplished using the 19 meter Space Ground Link Terminal antenna, with a gain of 73 dB, located in Las Cruces, New Mexico at the White Sands Testing Facility. To achieve the desired data rate, a 0.3 meter diameter antenna, with a gain of 31 dB, will be required onboard the spacecraft. With this size of onboard antenna, only a 10 W power draw is necessary in LDRO to transmit telemetry packets at the fixed 1 Mbps uplink and 5 Mbps downlink data rates.

For both uplink and downlink from Mars, the data rate will be fixed at 5 Mbps. This will be accomplished using the 34 meter Deep Space Network ground station antenna, with a gain of 77 dB, located in Goldstone, California, To achieve the desired data rate at the added distance and the use of the larger DSN antenna, SPrIntR will need to house

a 3 meter diameter antenna with a gain of 52.5 dB. For a 5 Sol Mars orbit, a 13 kW power draw is necessary to uplink commands and a 30 kW power draw is required to downlink telemetry at the fixed 5 Mbps data rate.

Both the 0.3 meter and 3 meter antennas will be high gain parabolic reflector antennas and a travelling wave tube amplifier (TWTA) will be utilized for both missions. This data rate, power, and sizing information, as well as related supplemental information, is reflected in the link budget provided below.

Table 5. Preliminary Link Budget for Mission to the Moon.

Item	Symbol	Units	Source	Command (Uplink)	Telemetry & Data (Downlink)
Frequency	f	GHz	Input parameter	28	18
Transmitter Power	P	W	Input parameter	1.00E+01	10
Transmitter Power	P	dBW	10log(P)	10	10
Transmitter Line Loss	Ll	dBW	Input parameter	-2	-2
Transmit Antenna Beamwidth	theta_t	deg	Input parameter	2.5	4
Peak Transmit Antenna Gain	Gpt	dB	Eq. (13-20)	73.32	36.3
Transmit Antenna Diameter	Dt	m	Eq. (13-19)	19	0.3
Transmit Antenna Pointing Offset	e_t	deg	Input parameter	0	1.2
Transmit Antenna Pointing Loss	Lpt	dB	Eq. (13-21)	0	-0.09
Transmit Antenna Gain (net)	Gt	dB	Gpt + Lpt	73.32	36.21
Equiv. Isotropic Radiated Power	EIRP	dBW	P + Ll + Gt	81.32	44.21
Propagation Path Length	S	km	Input parameter	3.84E+05	3.84E+05
Space Loss	Ls	dB	Eq. (13-23a)	-233.0797851	-224.1366245
Propagation & Polarization Loss	La	dB	Fig. 13-10	-0.2	-0.3
Receive Antenna Diameter	Dr	m	Input parameter	0.3	19
Peak Receive Antenna Gain (net)	Grp	dB	Eq. (13-18a)	36.29921262	68.49414902
Receive Antenna Beamwidth	theta_r	deg	Eq. (13-19)	0.15	3.9
Receive Antenna Pointing Error	e_r	deg	Input parameter	0.02	0.4
Receive Antenna Pointing Loss	Lpr	dB	Eq. (13-21)	-0.01777777778	-0.01051939513
Receive Antenna Gain	Gr	dB	Grp + Lpr	36.28143484	68.48362962
System Noise Temperature	Ts	K	Table 13-10	763	424
Data Rate	R	bps	Input parameter	1.00E+06	5.00E+06
Eb/N0 (1)	Eb/N0	dB	Eq. (13-13)	24.07862657	23.58312713
Carrier-to-Noise Density Ratio	C/N0	dB-Hz	Eq. (13-15a)	84.07862657	90.57282717
Bit Error Rate	BER	-	Input parameter	10^-7	10^-5
Required Eb/N0 (2)	Req Eb/N0	dB	Fig. 13-9	11.3	9.6
Implementation Loss (3)	-	dB	Estimate	-2	-2
Margin	-	dB	(1) - (2) + (3)	10.77862657	11.98312713

This figure includes information about both uplink and downlink communications for the specified mission. This is defined by input parameters and calculated values. Input parameters include values such as the operating frequency, transmitter line loss, propagation path length, receive antenna diameter, data rate, and bit error rate. The operating frequency reflects the appropriate Ka-Band frequency for downlink and uplink, based on recommendation from *SMAD: The Third Edition*, which will further be referred to in this section simply as *SMAD* [16]. Note that the transmitter power was determined using the MATLAB antenna sizing tool, as discussed in the next section, and the propagation path length is defined as the distance of transmission, which is equal to the Earth-Moon distance in Table 5.

To support this architecture, SPrIntR's communications hardware was selected. At a minimum, it was determined, mostly through reading *SMAD*, that an antenna, an amplifier, a transmitter/receiver, a phase modulator, and an oscillator were necessary to have a complete communications system. With this in mind, hardware was researched with the intent of creating a trade space. However, for Ka-Band specifically, there did not appear to be more than one option for each of the components listed above. Therefore, no trade study was actually conducted.

The hardware chosen includes a 0.3 m diameter High Performance Parabolic Antenna designed to function at the desired operating frequency of 28 GHz, as well as a Travelling Wave Tube Amplifier (TWTA) that is also capable of operating at 28 GHz. The TWTA is also the piece of hardware which sets the transmission efficiency at 55%. Next, a Ka-Band VSAT Transceiver was chosen to handle both the transmitter and receiver roles. Nominally, the transceiver transmits at a frequency of 28 GHz and receives at 18 GHz, which is expected for Ka-Band. Lastly,

Ka-Band QPSK Phase Modulator, as well as a Voltage Controlled Oscillator, were chosen. These are also meant to operate in the Ka-Band frequency range, although the listed operating frequency does appear to be slightly higher than that of the others. For the extendability requirement, a 3 m diameter High Performance Parabolic Antenna was also chosen for utility at Mars. Presented in Table 6 is a table of information gathered from each component's respective data sheet.

Table 6. Hardware Selection for SPrIntR Communications.

Component	Operating Frequency	Gain	Dimensions (mm)	Mass (kg)	Power	Volts	Current (mA)	Efficiency (%)
High Performance Parabolic Reflector Antenna, Single-polarized (Radiowaves)	27.3 - 31.3 GHz	36.5 dBi	542.3 x 308.6 x 406.4	7.7	Calculated transmit power: max 10 W at Moon	-	-	55
Space Traveling Wave Tubes (TWTs) - 99xxH	22-42 GHz	-	-	-	10 - 200 W	-	-	55
XRC33F16CD Value Enterprise Ka-Band VSAT Transceiver (TX)	IF Input Frequency Range 950 1450 MHz RF Output Frequency Range 29.5 30.0 GHz Local Oscillator Frequency (Nominal) 28.55 GHz	Conversion Gain, Linear Operation: 52-58 dB	204.4 x 77.8 x 121	1.8	RF Output Power, P1dB 34.5 dBm	(Supply) 15-50 V	(Supply) 1000-1500	-
XRC33F16CD Value Enterprise Ka-Band VSAT Transceiver (RX)	RF Input Frequency Range 19.2 20.2 GHz IF Output Frequency Range 950 1950 MHz Local Oscillator Frequency (nominal) 18.25 GHz	Conversion Gain: 50-62 dB	204.4 x 77.8 x 121	1.8	Max power: 2.25 W, Min power: 1.8 W (calculated)	(Supply) 9-25 V	(Supply) 200	-
Ka-Band QPSK/BPSK Phase Modulator	29 to 32 GHz	-	2.6 x 2.17 x 0.1	5*	~0 mW, Max Input Power Levels < 23 dBm	Vgs = 0 to 4.5 V, Vds = 0 V,	~0	-
Ka Band Voltage Controlled Oscillators	34 GHz	-	19.05 x 10.541 x 33.274	5*	output 15 mW	4-6 V	350	-
High Performance Parabolic Reflector Antenna, Custom (Antesky)	26.5 - 40 GHz	50.8 dBi	3000 diameter	36*	Calculated transmit power: max 30 kW at Mars	-	-	55

The components selected for hardware include a 0.3 m High Performance Reflector Antenna from Radiowaves, a Travelling Wave Tube Amplifier from L3, the XRC3F16CD Value Enterprise Ka-Band VSAT Transceiver from Skyware Technologies, a Ka-Band QPSK/BPSK Phase Modulator, a Ka-Band Voltage Controlled Oscillator from Microsemi, and a 3 m custom High Performance Parabolic Reflector Antenna from Antesky [17-20]. From Table 6, it is clear that several key elements of the data are missing, such as operating voltage and current for several of the components. Although this information was not included on the data sheet for some components, an extrapolation of these values from existing hardware for other frequency bands can be conducted in the future to estimate potential values for the missing data in the table. It is also important to note that the 3 m parabolic reflector antenna from Antesky would need to be a custom order, as only models for C and Ku-band are readily available [21].

c. Selection Criteria & Reasoning

In order to begin development of the communications subsystem, certain key variables needed to be determined, notably the desired data rate, operating frequency, and ground station antennas. The primary value of interest is the data rate. As stated, a 5 Mbps data rate is targeted for a majority of the communications capabilities, noting the exception of the 1 Mbps uplink capability at the Moon. This is due to the fact that likely much more information will need to be downlinked than uplinked, including detailed health and status of SPrIntR. Although 5 Mbps is likely much more than is needed, having the margin available to downlink pictures, for example, is an added benefit that could potentially assist other goals in the future. Secondly, Ka-Band was chosen for this architecture due to the fact that S-Band is becoming increasingly crowded and therefore unable to support additional high data rate missions [1]. Ka-Band is also best suited to handle such high data rates without needing to utilize any video uplink and downlink. An example of a mission that used Ka-Band for this exact reasoning is the Mars Reconnaissance Orbiter. Lastly, the ground station antennas were chosen because of SPrIntR GNC's use of the TDRSS system in cis-lunar space and the DSN en-route to Mars. The antenna chosen for lunar communications is a Ka-Band antenna used primarily for TDRSS purposes and the antenna chosen for martian communications is a dedicated DSN antenna.

With these initial variables determined, the next steps in the communications design are to select a transmit power and onboard antenna size. The latter is accomplished through a tool, written in MATLAB, that was designed to take inputs such as the chosen operating frequency and its corresponding wavelength, the assumed efficiency of the transmission, and possible antenna diameters. Using these inputs, the tool then calculates the range of possible antenna gains corresponding to the antenna diameters selected by the user.
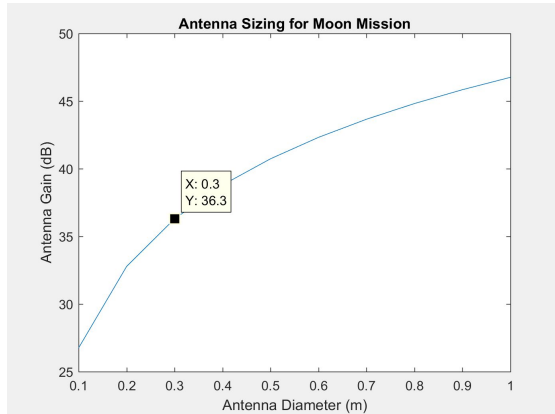
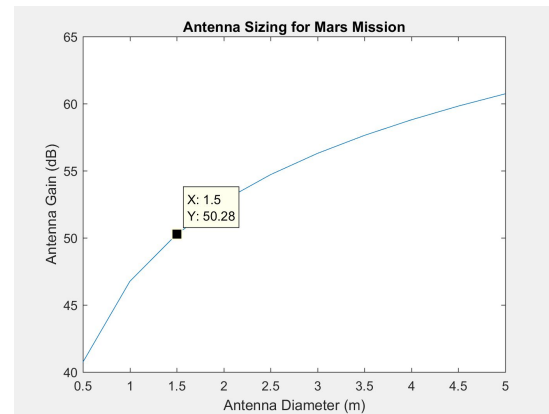**Fig. 11 Antenna Sizing for Moon Mission.**

Fig. 12. Antenna Sizing for Mars Mission

Both figures utilize Ka-Band as the operating frequency and assume 55% efficiency in transmission, regardless of uplink or downlink use. The main difference between Figures 11 and 12 is therefore the distance over which the signal needs to propagate. Figure 11 represents a distance between the Earth and the Moon of 384,400 km, while Fig. 12 represents a mission with a distance between the Earth and Mars of 3.99×10^8 km. This is important to note when selecting an antenna gain and size because the further the transmission distance, the larger the gain and diameter of the onboard antenna will need to be to overcome attenuation and free-space path losses.

In order to assist the rest of the communications design, antenna gain and size, as well as transmit power, is selected at this time. However, it is important to note that this will likely need to be adjusted later in order because these factors are arguably the most important in ensuring a positive link margin for each mission. From the plots, it was determined that a 0.3 meter diameter antenna, with a 36.3 dB gain, would be a good initial selection for SPrIntR for a lunar mission. This is because a 0.3 meter diameter antenna can easily be purchased in a environment (e.g. it's much more common to find 1 foot diameter parabolic dishes than it is to find 1.47 foot ones). An estimate of 5 W of power is initially selected for this mission, as it is known that cis-lunar communications will not require much power, especially compared to communications at Mars. For a mission to Mars, a 1.5 meter diameter antenna was chosen as the initial selection, with a 50.28 dB gain. This is because it is known that for the longer distance, a higher gain is needed. The initial estimated power draw is chosen at 10 kW. After the rest of the values needed for the link budget are calculated, these values will be visited again in order to guarantee positive link margin.

Following the development of the antenna sizing tool, the aforementioned free-space path losses for communication at the Moon and at Mars were calculated. Free space loss is a measure of the loss of a signal's strength over the distance in which the signal propagates, assuming there are no major obstructions in the path. For downlink from the Moon, the space loss was determined to be -187.1 dB and for downlink from Mars, the space loss was -332.3 dB. This is a rather significant amount for Mars communications and exemplifies the need for a larger onboard antenna gain, and therefore a larger sized antenna, in order to counteract the loss.

Before that was done, however, a modulation scheme was chosen for SPrIntR. Using Fig. 13-9 from *SMAD* the theoretical Signal to Noise Ratio per bit was found.

SNR was calculated using the maximum fixed data rate of 5 Mbps and a bandwidth of 18 GHz for downlink in Ka-Band. Applying this value resulted in a E_b/N_0 = -1.6. This is very close to the Shannon Limit from *SMAD*. This is because, in designing the communications subsystem, ideal conditions were assumed for theoretical calculations, as the team does not have access to an actual signal sample that had propagated from the Moon to Earth or vice versa. Therefore, in order to appropriately choose a modulation scheme, the decision needed to be approached from a qualitative standpoint, rather than a quantitative one. Several modulation schemes were considered for their pros and cons and the scheme that benefitted SPrIntR most was chosen. First, Binary Phase Shift Keying (BPSK) was considered. This scheme is characterized by its ability to provide the maximum power efficiency of any modulation scheme. However, it is also the most simplistic of them, meaning that for more complicated signal analysis, BPSK

27

would not be a good match. Next, Quadrature Phase Shift Keying (QPSK) was considered. This modulation scheme produces a very similar power efficiency to that of BPSK, but also allows for twice the data rate of BPSK, as the bandwidth of QPSK is generally narrower. Although in research, it was not made explicit what range of data rate is supported by BPSK, it can be assumed that since twice of any range provides more options, that must be a benefit for QPSK no matter the original data rate range. Next, Gaussian Minimum Shift Keying (GMSK) was considered. This modulation scheme was deemed the best for high data rates, though again what "high data rate" refers to exactly is not explicit. However, the power efficiency is rather poor. Lastly, Frequency Shift Keying was considered. This modulation scheme is characterized by the fact that it can be specialized for a given frequency range. Similarly to GMSK, however, it also has fairly poor power efficiency and is very difficult to implement. After weighing all the pros and cons of these various modulation schemes, it was determined that QPSK would be the best for SPrIntR's communications system. This is because QPSK seems to be more flexible than BPSK while still being relatively easy to implement, as our signal is not anticipated to be complicated. Although GMSK was the best scheme for high data rates, which SPrIntR may be considered having, the detriment to the power efficiency outweighs the benefit of achieving the highest data rates with ease. SPrIntR's high power requirement dictates that the best case scenario would more often than not include the option of the best power efficiency. Therefore, BPSK was chosen [1].

Several values in the link budget were extrapolated from tables and figures in *SMAD*, while others were assumed based on logic presented in the example from the book. The system noise temperature was extrapolated from Table 13-10 in *SMAD*.

Additionally, the required SNR per bit was assumed through the use of Fig. 13.9 in *SMAD*. The propagation and polarization loss was determined by finding the attenuation that corresponds to the chosen uplink and downlink frequency in Fig. 13-10 from *SMAD*.

Values like the transmitter line loss and bit error rate in Table 5 was assumed based on recommendation from *SMAD*. The example given in the book references satellite communications in Low Earth Orbit (LEO). Given that a detriment of 3 dB was assumed for LEO, an optimistic assumption was made that only 3 dB of loss would occur at distances of the Moon and Mars. However, the inclusion of free space losses likely counteracts any overly conservative assumption made in regard to the transmission line loss. Due to the fact that all communications calculations in this report are purely theoretical, the bit error rate (BER) assumed is the same in Table 5 as they are in *SMAD*'s example, which could further reflect an overly conservative estimation. Error in the BER assumption would likely also be corrected, in this case by the calculation of the SNR per bit calculation, which will be discussed ahead [1]. Lastly, the implementation loss, a measure of the overall distortion or phase noise encountered in transmission, was assumed to be equal to that experienced by the communications satellite from the example in the book [22].

It is at this point that the transmit power and antenna gain and sizing are revisited. After calculating every other value necessary to achieve a complete link budget, the initial antenna gain and size selected for both the Moon and Mars from the antenna sizing exercise described above leaves a negative margin. This is either due to a selection of transmit power that was too low or a selection of antenna gain and sizing that is too low. These values are then adjusted on a trial-and-error basis using the link budget tool as a guide until each margin is positive. The final result is checked to ensure that the transmit power chosen is within the realm of reason for SPrIntR and that the antenna size is not so large that it cannot fit within the rocket fairing for launch. The final result culminating in positive link margins all around is presented in Table 7 below.

Table 7. Antenna Sizing and Transmit Power Chosen Resulting in Positive Link Margin.

Mission Case	Moon	Mars
Uplink	Antenna diameter: 0.3 meters Transmit Power:10 W Link Margin: +10.78 dB	Antenna diameter: 3 meters Transmit Power: 13 kW Link Margin: +4.66 dB

Downlink	Antenna diameter: 0.3 meters Transmit Power: 10 W Link Margin: +11.98 dB	Antenna diameter: 3 meters Transmit Power: 30 kW Link Margin: +5.37 dB

To conclude the design of this architecture, SPrIntR's communications hardware was selected. Although the recommended, hardware was researched with the intent of creating a trade space, for Ka-Band specifically there did not appear to be more than one option for each of the components *SMAD* suggested. This includes both the 0.3 m and 3 m antennas, the amplifier, transmitter/receiver, phase modulator, and oscillator. Therefore, no trade study was actually conducted.

7. *Thermal*
a. Flow Down From Top-Level Requirements
The thermal requirement for SPrIntR is based on the mission mandate requirement of operating with 200 kW of power for LEO to LDRO and 500 kW of power for Mars. This requirement will require that the SPrIntR can radiate excess heat generated from onboard electronics and propulsion systems for its life cycle. There are two types of thermal control methods, active and passive. Passive thermal control is based on the surface properties of the spacecraft rather than active thermal control, which relies on a designed thermal control system, powered by the spacecraft. SPrIntR will have both passive and active thermal control. Proper temperature control within SPrIntR is critical to the success of the mission, because every component of the payload and the spacecraft bus has required temperature limitations. These requirements may include an operation and a survival temperature range, which, if exceeded, may result in reduced performance and/or permanent damage to the component. Electrical devices will not work properly or may have a shortened life span if they overheat. Battery efficiency decreases if the temperature is off nominal or if there is a significant temperature difference between battery cells. Liquid hydrazine will freeze in the fuel lines if it gets too cold, making it impossible to get fuel to the thrusters. Large temperature gradients can also deform the spacecraft structure, possibly leading to significant pointing errors. These are just a few of the mission-ending problems that may occur if temperatures are left uncontrolled [23].

b. Selected Architecture
The selected architecture consisted of covering the bus in MLI with the surface layer being of aluminized kapton and the interior layers are doubly-aluminized kapton which is commonly done to passively control temperatures since MLI blankets prevent both excessive heat loss from a component and excessive heating from environmental fluxes, rocket plumes and other sources. Radiators would be covered in magnesium oxide aluminum oxide paint due to its extremely low absorptivity and high emissivity and the sizing would be 19.2 m^2 for LEO to LDRO which will remove heat from the bus and the PPUs and 51.51 m^2 for Mars which just needs to remove heat from the PPUs since the surface area for Mars SPrIntR is significant enough to remove excess heat from the bus. NASA typical wants areal densities for radiators to be between 2-4 kg/m^2 therefore the mass for the Lunar mission radiator would be approximately 40 kg and for the Mars mission radiator would be 105 kg [24]. Would need to look into heaters for at Mars, since analysis was only done for Mars' SPrIntR at Earth.

c. Selection Criteria & Reasoning
i. *PDR Iteration*
Based on the methods SME, an average temperature requirement for bus of the SPrIntR was found based on required operating temperatures of each subsystem. Table 8 of the averaged required temperatures can be found below.

Table 8. Operation Temperatures

Subsystem	Average operating temperature (K)
Avionics	293
Batteries	293

Hydrazine tanks	300.5
Xenon tanks	310.5
Overall bus average required	299.3 ± 10

From the above table, an overall required bus temperature was found to be 299.3 K. This value is at a plus or minus of 20 degrees Kelvin due to average operating temperatures for all of the listed subsystems falling within those ranges. Using this estimated value the first iteration of the thermal subsystem can be estimated as a cubic point with a temperature of 299.3 K. One side of the rectangle is will be assumed to face the sun at all times and every side of the cube will be radiating heat from its surface.

The heat energy that is entering SPrIntR's bus was estimated based on the initial power requirements as well as the incident solar radiation which it will be experiencing on average. The power that is dissipating through SPrIntR's electronics and propulsion system was estimated to be 25% of the power entering the system. This estimate means 50 kW of energy are entering the bus that need to be radiated into space. In addition, the solar heat energy was calculated to be 9835.2 W, this value was estimated using the properties of the Z93 white paint. The Z93 white paint was chosen due to its high emissivity and its low absorptivity, from the selections within SME it was the best option. These calculations can be seen below.

$$Q_{in_{solar}} = S\alpha A_p = 9835.2 \ W \tag{14}$$
$$Q_{in_{total}} = Q_{in_{solar}} + Q_{in_{power}} = 59835.2 \ W \tag{15}$$

Using the total heat into the system, a requirement was met of how much heat needed to be extracted from the bus using radiators.

$$Q_{in} = Q_{out} = \sigma T^4 \varepsilon A_{rad} \tag{16}$$

Using the equation for heat lost through radiation, the required area to keep SPrIntR at an average temperature of 299.3 K, while using the Z93 white coating was found to be 143.5 meters squared. The values for the minimum and maximum temperatures were also computed, these values can be found below.

Table 9. Required Area for Heat Transfer

Temperature (K)	Area needed to achieve desired temperature (m^2)
289.3 (minimum)	163.5
299.3 (average)	143.5
309.3 (maximum)	125.33

As can be seen above, the allowable areas needed for operations range from 125-163.5 meters squared. If these numbers are compared to SPrIntR's bus structure which has a total area of 90 meters squared it can be seen that SPrIntR does not have enough surface area to self-radiate the excess heat. Therefore, two radiator arrays were added to the central structure of SPrIntR. The arrays will be made of the same Z93 coated aluminum as the structure and will be cooled using an ammonia piping system to transfer heat to the panels. Each array will be 16 meters long and 2 meters wide, there will be a total of 4 panels in each array. This will allow for the 59835.5 W of energy to be radiated into the space around the SPrIntR. These arrays will not allow the structure to ever reach its minimum temperature but will ensure that the maximum and average temperature is achievable.

This iteration was an overestimate since this looked at total heat dissipation, did not take into account that the radiator dissipates heat from both sides and only considered heat energy from solar and not Earth's infrared and

30

albedo. This was a very basic back of the envelope calculation and as roles changed in the team, the thermal design started from scratch and was further looked into.

ii.   Current Iteration

Heat Dissipation

    A more in depth analysis was used to determine temperatures of SPrIntR. The process consisted of subdividing the system into "properly sized" chunks (nodes) and wire them together thermally acquiring a system of differential equations. The following were made into thermal nodes to make the thermal analysis not overly complicated, but also gives a reasonable output: Solar arrays, bus, payload, PPUs, and thrusters. Which can be solved given appropriate initial and/or boundary conditions. For the analysis performed these initial conditions and/or boundary conditions consisted of an estimated initial temperature of the spacecraft which was assumed to be 20ºC and the boundary conditions for the final analysis was from environmental heat loads at various altitudes and heat dissipations from each of the thermal nodes in which 175 kW was designated to propulsion and assumed 5 kW is being dissipated from the bus with the remaining 25 kW of power just using an educated guess of an efficiency of 80%. There is less than 10% heat rejected radiatively from sides and top for the PPUs which was multiplied by the power going into propulsion for the heat dissipation of the PPUs and the remaining power would go to the thrusters which have an efficiency of 72% [24].

Thermal Environment

    The thermal environment for heat energy due to solar flux in watts was calculated using the following equation:

$$Q_{sol} = G_s A \alpha (1 - f) cos(\beta) \tag{17}$$

    The beta angle in degrees, β, was calculated using the analysis done in section 3.2 except changes were made to account for the correct efficiency of the NEXT propulsion system of 72% instead of 75% and input power of 175000 instead of 100000 which only produce minor changes in the final temperatures by ±4ºC. Also, the eclipse fraction, f, was also calculated using what was developed in section IV - B. The eclipse fraction represents the fraction of an orbital period that the craft will be in eclipse. Therefore 1-f would be the fraction in which SPrIntR is in the Sun. G_s is the solar flux which was taken to be the average value for the final analysis (1367 W/m^2) except for sizing the radiators, which will be later discussed of why that is. A is the area of the body in m^2 that is pointing directly at the Sun by assuming the solar rays as constant vectors around the changing orbits. α is the absorptivity of the body facing the Sun which is characterized by its material property.

Conductances

    Conductance between nodes was calculated using the basic conduction equations. The thermal capacity, C in W/K, between the nodes were based on educated guesses since conductance can be hard to calculate directly without knowing the exact physical connections between each node. Values were used that would assume moderate to well insulated material for the size of SPrIntR since a docking ring should be a poor conductor and a well insulated material between the bus and the payload, the bus and the PPUs, and the PPUs and the thrusters since that could cause the bus to get extremely hot since it is thermally connected amongst 4 other nodes. Since the solar panels are large and relatively far from the bus, it should be expected that the conductance does not make much difference.

Radiation

    The final heat load that is taken into account was radiation which was also used to size the radiator. Since a radiator uses a high emissivity and low absorptivity to remove heat which typically is just white paint. The basic radiation equation is:

$$Q_{rad} = \sigma A \, \varepsilon \, F \, T_{obj}{}^4 \tag{18}$$

    Where σ is the Stefan-Boltzmann constant in W/[m^2-k^4], A is the surface area in m^2, ε is the emissivity of the surface, F is the view factor to space, and T_{obj} is the temperature of the object or surface in kelvin. Surfaces can also radiate to other surfaces and not just space, which is where the view factor, F, comes in. A lot of assumptions were made for the view factor to simplify the analysis. Such as the solar arrays are thin and perfectly facing the Sun allowing for the two sides of the bus where the two solar arrays attach to have a view factor of 1 to space meaning

31

that the sides cannot see the solar arrays and shouldn't radiate onto the arrays. An important symmetry relationship exists between the two view factor fractions between two different surfaces [25]:

$$A_i F_{i-j} = A_j F_{j-i} \qquad (19)$$

The view factor, F_{i-j}, is defined as the fraction of radiation emitted by surface i that is intercepted by surface j. Similarly, F_{j-i} would be the fraction of radiation emitted by j that is intercepted by i. A_i is the surface area of surface i and A_j is the surface area of surface j both are in m^2. Since all the nodes are on top of one another the easiest way to find the view factor is to divide the smaller area by the bigger area which will be the view factor of the larger area object to the smaller area object and since view factors must add up to one, the missing view factor is just one minus this which the missing view factor was assumed to be space. After the view factor between two surfaces is found then the heat flow (Q_{ij}(W)) from surface i to surface j can be calculated using this equation:

$$Q_{ij} = \frac{\sigma(T_i^4 - T_j^4)}{\frac{1-\epsilon_i}{A_i \epsilon_i} + \frac{1}{A_i F_{i-j}} + \frac{1-\epsilon_j}{A_j \epsilon_j}} \qquad (20)$$

T_i is the temperature of surface i in kelvin, T_j is the temperature of surface j in kelvin, ϵ_i is the emissivity of surface i, and ϵ_j is the emissivity of surface j. This is assuming that the two surfaces form an enclosure, meaning that none of the radiation is lost to other surfaces or to space.

Now that all the heat loads are figured out, the next step was constructing the system of differential equations for each node. Which the governing equation here is the first law of thermodynamics for a closed system with no work done. The quantity mC_p is mass multiplied by the specific heat capacity in J/k, can be referred as the thermal mass of the node. The thermal mass has no effect on the steady state value, it only affects the time it takes to reach steady state. Which means estimated values are fine for this analysis especially since this is electric propulsion and the transfer takes a long time. From structural analysis and research, the mass values were estimated for each node and specific heat for each node was approximated by using the specific heat value for gallium arsenide for the solar arrays, taking a weighted average for the specific heat of the bus using xenon and magnesium AZ1 alloy, same kind of weighted average was done for the payload, PPUs were just assumed to be made out of aluminum, and the thrusters were assumed to be made out of stainless steel.

Material properties for each node was analyzed by assuming the bus would be covered in MLI since this is commonly done to passively control temperatures since MLI blankets prevent both excessive heat loss from a component and excessive heating from environmental fluxes, rocket plumes, and other sources. The common MLI blanket has a surface layer of aluminized kapton which has a solar absorption $\alpha = 0.35$ and an IR emissivity of $\epsilon = 0.7$ and the interior layers are doubly-aluminized kapton, and these layers (interior and inner) have an emissivity of $\epsilon = 0.03$. This would be an ideal for a hot case which should be expected for substantial amounts of heat dissipation. Since the bus is fairly smooth being a rectangular box the effective emissivity of 0.03 should be valid.

In order to figure out the temperature of the MLI blanket would need to use the previous values of the temperature of the object and iterate through. The outer layer of the blanket will still follow normal heat loading due to the environment and radiating off heat using the outer layer solar absorption and IR emissivity.

The material properties for the solar arrays on the top side that has the solar cells was assumed to have a solar absorption $\alpha = 0.9$ and an IR emissivity $\epsilon = 0.9$ which was found that most solar cells have an $\alpha = \epsilon$ relationship. [1] For the backside of the solar panel that is facing back towards Earth, this can typically be painted black or white depending on heating or cooling, due to the size of the solar arrays this was painted white in order for the solar arrays not to get too hot. The white paint used was magnesium oxide aluminum oxide paint due to low absorptivity $\alpha = 0.09$ and high emissivity $\epsilon = 0.92$ which was also chosen for the radiators for the same reasons. For the payload this can vary based on the customer needs which is evaluated in SPrIntR's user guide in the payload module section . For the initial calculations assumed a solar absorption $\alpha = 0.9$ and an IR emissivity $\epsilon = 0.9$. PPUs were assumed to act as a heater enclosed in the bus therefore emissivity and absorptivity are irrelevant. The thrusters are made from stainless steel which has a solar absorptivity $\alpha = 0.47$ and an IR emissivity $\epsilon = 0.14$.

The sizing of the radiator was calculated by the assumption that the PPUs act as a heater that constantly dissipates heat from the propulsion system. Since the PPUs dissipate more heat than the bus, the radiator can also be used to remove heat from the bus. The calculations were done by treating the radiator as a flat plate with the hottest case in which one side of the radiator faces directly at the Sun and the other side faces the Earth. This is using a solar

flux of 1414 W/m² to ensure hottest case possible. The albedo and Earth's infrared are taken at an altitude of 400 km since these affects diminish at higher altitudes and also assuming that the spacecraft is in the Sun 68% of the time using the maximum Beta angle. The area of the radiator comes out to be 19.2 m². The results help confirm that the PPUs stay at operating temperatures using this size radiator to remove heat.

Table 10. Power Processing Unit Key Characteristics.

Mass, kg	34.5	
Envelope, cm	41.9 x 52.1 x 14.0 (excl. connectors, feet and screw heads)	
Input Power, W	610 - 7220 (unreg 80-160 VDC high power bus) 28 max. (22-34 VDC low power bus)	
Electrical Interface	Input 80-160 VDC	D38999/20GC11PN (11 lines)
	Input 28 VDC	D38999/20GA94PN (2 lines)
	DCIU Slice I/O RS-485	SDD15F402 (D-sub-min 15 contacts)
	Output Neutrlzr	D38999/20GD5SN (3 lines) 2X
	Output Thruster	Modified D38999/20GJ8BN (7 lines) 2X
Thermal Interface	Baseplate: -20 to +65°C operating -40 to + 70°C non-operating Less than 10% heat rejected radiatively from sides and top	
Structural capability	Static	22 g
	RandomVib	14.1 g_{rms} qualification
	Pyroshock	2000 g peak

There is also operating temperatures for the bus which was taken to be the upper limit for batteries since they have the smallest margin of operating temperatures and lowest upper limit. This was found from SME to be 30ºC. The hydrazine fuel has the highest lower limit for operational temperatures which also needs to be taken into consideration which was found from SME to be 15ºC. [1]

Results

Used the radiator to dissipate heat from the bus as well since the temperatures were too high for allowable flight temperature and added a way to predict the steady state temperatures of the spacecraft at various altitudes in transfer orbit. This was done using eqns 88-93 to calculate the beta angle and eclipse fraction at each altitude. Also, used eqns 66-70 to predict heat flux due to Earth's albedo and infrared which helped show that those effects are negligible at higher altitudes.

Table 11. Temperatures for Each Node at Various Altitudes.

Altitude (km)	Solar Array 1 (ºC)	Solar Array 2 (ºC)	Bus (ºC)	Payload (ºC)	PPUs (ºC)	Thrusters (ºC)
400	36.29	36.29	13.55	3.86	55.23	226.42
10360	48.57	48.57	22.73	2.86	45.94	224.66
20320	53.01	53.01	27.24	5.95	45.15	224.47
30280	48.55	48.55	22.71	1.94	44.24	224.38
40240	53.42	53.42	27.74	6.04	44.62	224.38
50200	50.13	50.13	24.31	3.17	44.16	224.35
60160	53.33	53.33	27.62	5.90	44.48	224.35
70120	55.21	55.21	29.50	7.47	44.66	224.36
80080	53.39	53.39	27.67	5.93	44.43	224.34

33

| 90040 | 55.59 | 55.59 | 29.90 | 7.80 | 44.67 | 224.35 |
| 100000 | 56.35 | 56.35 | 30.67 | 8.46 | 44.75 | 224.36 |

As seen in Table 11 for the temperatures at various parts of SPrIntR, the solar array temperatures generally increase as altitude increases, but some decrease due to the beta angle changing and eclipse fraction changing since those are not a linear relationship. Initially the bus temperature is below the requirement for hydrazine of 15℃, but this can easily be addressed by decreasing the radiator area by retracting in the radiator and then extending it back out when needed. Also, at highest altitude the temperature for the bus is 30.67℃ which is slightly above the requirement for the batteries of 30℃, but that is the operational temperature and since the eclipse fraction is negligible at higher altitudes the batteries would not need to be operating and would still be within their survival temperature.

The payload temperature is within 4℃ - 9℃ which is due to not including a heat dissipation in the payload which is good since this can allow to do a trade study of figuring out what's the allowable heat dissipation given various α/ε ratios, the current iteration used an α/ε ratio of 1. The largest α/ε would dictate the lowest heat dissipation that can be applied by the payload while the lowest α/ε would specify the highest heat dissipation of the payload, which is only considering the max allowable flight temperature since heat dissipation is going into heating the payload and not cooling. There is a correction of the payload module to make the temperatures higher by insulating the top and bottom of the max allowable payload in order for those surfaces to not radiate off heat which is shown in SPrIntR's User Guide.

The prediction of sizing of the radiators using 55℃ is verified by seeing that the PPUs get to 55.23℃ at 400 km. Since the PPUs are enclosed inside the bus, the temperature is constantly decreasing and remaining constant seems to make sense since the PPUs are not exposed to the radiation environment and the radiators are being used to keep them at operational temperatures. The temperature of the thrusters remains at a constant 224℃ regardless of the thermal environment with different altitudes which could be due to the heat dissipation from the thrusters being much larger compared to the heat loads from the environment. Since the thrusters are made from stainless steel this high temperature should be maintainable and the thrusters being at the highest temperature is expected. From ref. [26] this seems to be reasonable which is mentioned that ion thrusters can reach temperatures as high as 300℃ during peak thrusting. The temperatures of the bus and solar arrays get hotter further from Earth due to the beta angle being at it's almost maximum and the eclipse fraction being zero which can be seen in section IV. B and the reason for the fluctuation is due to the beta angle constantly changing and the eclipse fraction changing by a margin.

In order to make better analysis of the temperatures in Table 12, typical temperature requirements were taken from SME [1] which can be found below which includes operational and survival temperatures that the PDR iteration did not include:

Table 12. Typical Temperature Requirements.

Equipment	Operational (℃)	Survival (℃)
Avionics Baseplates	-20 to 60	-40 to 75
Batteries	10 to 30	0 to 40
Hydrazine Fuel	15 to 40	5 to 50
Solar Arrays	-150 to 110	-200 to 130
Antennas	-100 to 100	-120 to 120
Xenon Tank	25 to 50 [3]	N/A

By looking at Table 12 there is problems at the low altitudes of 400 km and 10360 km for the bus for the hydrazine fuel and xenon tank which can be addressed by using heat from the PPUs to heat the bus instead of radiating most of the excess heat from the PPUs or by having the radiators remove less excess heat from the bus by reducing the area of the radiators for operation or extracting less heat from the bus by the radiators.

34

8.   Payload Subsystem
a.   Flow Down from Top-Level Requirements
    The only top-level requirement given from the mission mandate concerning the payload is shown below leaving the vision of the payload subsystem entirely to the SPrIntR team..
- The spacecraft shall be capable of safely transporting cargo between LEO and LDRO.

b.   Selected Architecture
    The design of SPrIntR's payload module has been approached with a "black box" perspective, with prospective clients (be it NASA or a private entity hoping to resupply a colony) responsible for its design, fabrication, packaging, and transport from Earth's surface to LEO. This allows for flexibility in achieving clients' mission goals and timelines, provided the client follows a set of mandated payload module requirements. These requirements have been outlined in a "SPrIntR User's Manual", similar to the existing user's manuals of commercially available launch vehicles. Some example payload module requirements include a maximum wet mass, maximum envelope size, mandatory center of mass window, docking interface compatibility, and low Earth orbital parameters. Once the payload module has achieved LEO and is ready for transport, SPrIntR assumes full responsibility for rendezvous, capture, and transport to desired orbit. For the purpose of ADCS (Attitude Determination & Control System) calculations and other system integration considerations, the general architecture of the payload module has been modeled similarly to that of Orbital ATK's Cygnus Cargo Module.

    The payload module shall be no larger than 6 meters in diameter and 6 meters in length, and must be constructed with a NASA Low-Impact Docking System (LIDS) compatible docking interface. For the Lunar mission phase, the maximum cycle payload mass is 12,000 kg. For the Mars mission phase, the maximum cycle payload mass is 24,000 kg. The calculation of these masses is discussed below.

c.   Selection Criteria & Reasoning
    The overall mission mandate for the SPrIntR mission gave no requirements for payload mass, payload transport time, or propellant mass, leaving it to the SPrIntR team to develop a novel method to optimize these variables. This optimization maximizes the quantity (Transportation Rate)/(Required Propellant Mass), and is discussed extensively in Section II.C.3. The payload optimizations for the Lunar and Mars mission phases are given below.
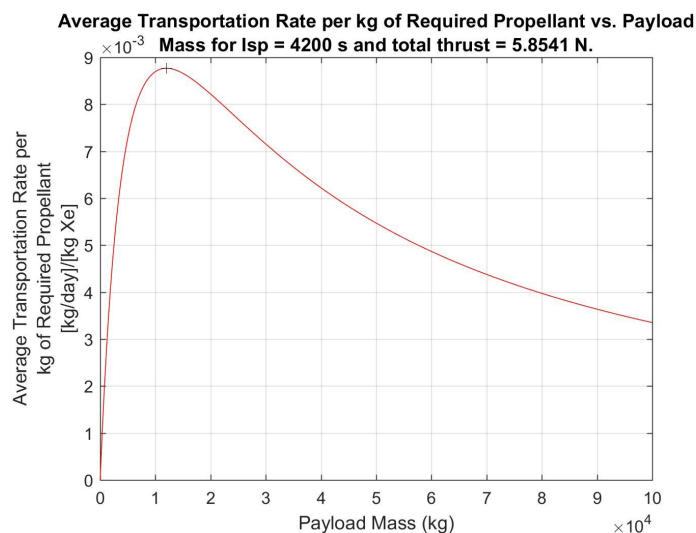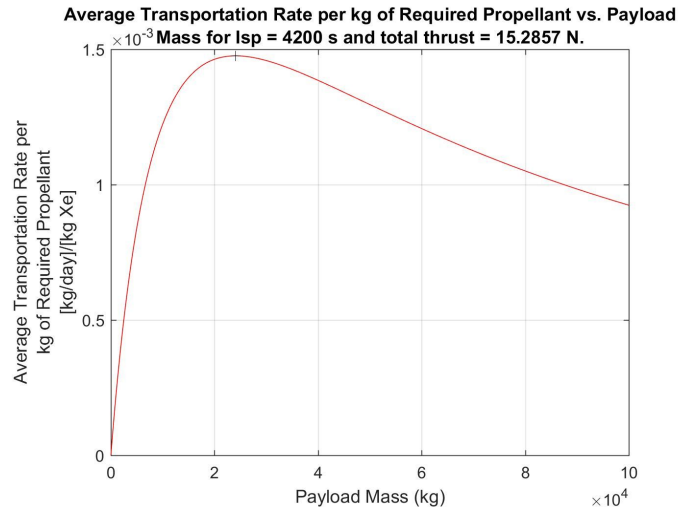

Fig. 13   Lunar Mission Phase Payload Optimization

Fig. 14   Mars Mission Phase Payload Optimization

D. Budgets

1. Delta-V

Because SPrIntR is an SEP vehicle, its delta-v budgets can be approximated by taking the difference of the initial circular orbit and the final circular orbit, and adding margins to account for orbital injections and attitude control. The delta-v required per cycle was calculated to be approximately 14 km/s for the Lunar mission and 32 km/s for the Mars mission.

2. Power

Table 13. Lunar Mission Phase Power Budget.

Subsystem	Draw [W]
Propulsion	0-180,000
Power	8,000
Structures/Mechanisms	0-500
ADCS	0-480
GNC	0-92.7
Communications	0.8-9,860
Thermal	TBD
Total	200000

Table 14. Mars Mission Phase Power Budget.

Subsystem	Draw [W]
Propulsion	0-470,000
Power	15,000
Structures/Mechanisms	0-500

36

ADCS	0-480
GNC	0-92.7
Communications	0.8-9,860
Thermal	TBD
Total	500000

3. Mass

Mass budgets were documented using an automated Microsoft Excel spreadsheet that was continually updated throughout the design phase. The total wetted mass for the Lunar mission is 28336 kg, and the total wetted mass for the Mars mission is 46990 kg.

4. Cost

SME [1] has given several linear regression models that can be used to estimate the initial development cost of space missions. These models are constructed using available data from historic and current space missions, and are adjusted for inflation. The models take inputs such as spacecraft size, mass, operating power, mission purpose, lifespan, and many others. Using an average of several of the most applicable models, SPrInt's initial development cost is estimated to be in the budget range of NASA's Large Strategic Science Missions, coming in at a minimum of $1 billion for the Lunar phase SPrIntR. The dollar amount for the structural and thermal subsystems is $88.93 and $0.91 million, respectively. The communication and propulsion subsystems cost of $5.20 million and $105 million, respectively. The power and ADCS subsystems have a cost of $97.77 and $41.13 million, respectively. For comparison, this represents nearly one third of the development budget for NASA's Space Launch System, about same the cost of the development of NASA's Curiosity Rover, and less than 1% of the projected costs associated with the U.S. military's development of the F-35 fighter jet. After production and manufacturing methods have been established for the Lunar mission configuration, the development costs for the Mars mission configuration should decrease.

SPrIntR's mission will also include yearly recurring costs associated with the acquisition of propellant and ground support personnel for each mission cycle. Using a high estimate of the current market Xenon gas price of $1200 per kg, a yearly 6000 kg propellant acquisition would represent $7.2 million in recurring propellant costs. Assuming a ground support staff of twenty salaried engineers, a high-end estimate for the personnel recurring costs comes to about $700,000 per year. Due to the modularity and possibility component replacement of the SPrIntR system, the mission is expected to last longer than 10 years. With the initial development costs included, the initial 10-year expenditure associated with the program would come to about $2 billion.

E. Operations & Ground Support

The operations & ground support of SPrIntR is fairly minimal and already in place due to other missions. During the Mars extensibility phase, SPrIntR will require access to NASA's Deep Space Network ground stations. During the LDRO phase, the NASA's TDRSS will relay data to a NASA ground station. These ground stations will have to support trajectory changes and some attitude control during mission critical phases like payload capture. During transient maneuvers, due to its non-critical nature, SPrIntR will operate autonomously. Therefore, SPrIntR will require daily or weekly check ups rather than constant monitoring from ground station personnel.

IV. Problem-Specific Design Solutions

A. Eclipses & Changing Power Schedule

SPrIntR is a fully solar electric powered reusable vehicle that will periodically encounter solar eclipses throughout its spiral out transfer orbit to the moon. As such, this requires some analysis regarding the craft's optimum secondary battery capacity and power scheduling both in and out of eclipse throughout its transfer orbit. This section outlines the analysis behind the craft's estimated average and maximum eclipse times and power scheduling.

The first challenge associated with our analysis is determining the exact eclipse time for which to size the craft's batteries and plan a power schedule for. Over its lifetime, the Sprinter will encounter eclipse times ranging anywhere from 25 minutes to 3.5 hrs, depending on the time of year, its current altitude, and its beta angle. With the power requirements of the craft, it becomes unreasonable to size the batteries for the possible but unlikely worst case eclipse of 3.5 hours, and objective determination of the "90%" case is required.

The beta angle (β) is the angle between the solar vector and its projection on the orbital plane. This angle is not static, and varies with time. Two main factors affect β, these are the change in seasons (variation in Ecliptic True Solar Longitude (Γ)) and perturbation of the orbit due to the oblateness of the planet (variation in Ω).

$$\beta = sin^{-1}[cos(\Gamma)sin(\Omega)sin(i) - sin(\Gamma)cos(\varepsilon)cos(\Omega)sin(i) + sin(\Gamma)sin(\varepsilon)cos(i)] \qquad (21)$$

In this equation [27], our spacecraft's inclination is assumed to be fixed with the Moon's 5.14 degrees, and ε is the Obliquity of the Ecliptic which for Earth is presently 23.45 degrees.
Geometrically, it can be shown that β is bound as the following:

$$\beta = \pm(\varepsilon + i) \qquad (22)$$

which for our present values is ± 28.59 degrees. This range will help to validate the present analysis. The change in Γ can simply be approximated by

$$\frac{d\Gamma}{dt} = \frac{2\pi}{365.25} \frac{rad}{days} = 1.99 \times 10^{-7} \ rad/s \qquad (23)$$

The variation in the Right Ascension of the Ascending Node depends on the craft's inclination and orbital altitude, and for a circular orbit is given by

$$\frac{d\Omega}{dt} = -\frac{3}{2}J_2\left(\frac{R_E}{h}\right)^2 \sqrt{\frac{\mu}{h^3}}cos(i) \qquad (24)$$

where J_2 is Earth's second dynamic form factor, R_E is the radius of Earth, μ is Earth's gravitational parameter, and h is the craft's orbit radius.

In this analysis, SprIntR's spiral-out transfer is approximated as a circular orbit whose radius is slowly growing one kilometer at a time at the same rate that the craft's propulsion system supplies the necessary ΔV to attain a one kilometer radius change. This time step is computed by using the ideal rocket equation (beginning with the current best-estimate of the craft's dry mass and payload mass, as well as an initial propellant mass of 7000 kg) to calculate the required propellant for each kilometer step, and then dividing that by the mass flow rate of the craft's propulsion system. For the purposes of this analysis, the power supplied to the propulsion system was fixed at 100 kW, and the mass flow rate was calculated using

$$\eta P_0 = \frac{1}{2}\dot{m}(I_{sp}g_0)^2 \qquad (25)$$

where η is the efficiency of the NEXT propulsion system (75%), I_{sp} is the specific impulse of the propulsion system (4200s), P_0 is the input power, and $g_0 = 9.81 \ \frac{m}{s^2}$. The timestep becomes smaller as the propellant is consumed, and the analysis accounted for this.

With the timestep now computed, the Ascending Node Angular Rate was computed over an increasing orbital altitude from 400 to 100,000 km using Eq. 4. The Ascending Node Angular Rates were then multiplied by their corresponding timesteps to find the change in the Right Ascension of the Ascending Node as the craft spirals out from earth. The same was done for the variation in Ecliptic True Solar Longitude.

For this analysis, it was assumed that the craft begins its transfer orbit on the Vernal Equinox ($\Gamma = 0$) with an inclination equal to that of the Moon's (5.14 degrees), and its Right Ascension of the Ascending Node equal to 360 degrees. With Γ and Ω known for each point in the transfer orbit, β can also be calculated for each point in the transfer using Eq. 93. The eclipse fraction at each point in the transfer, f, can now be calculated using

38

$$f = \tfrac{1}{\pi} cos^{-1} \left[\frac{\sqrt{h^2+2R_E h}}{(R_E+h)cos(\beta)} \right] \tag{26}$$

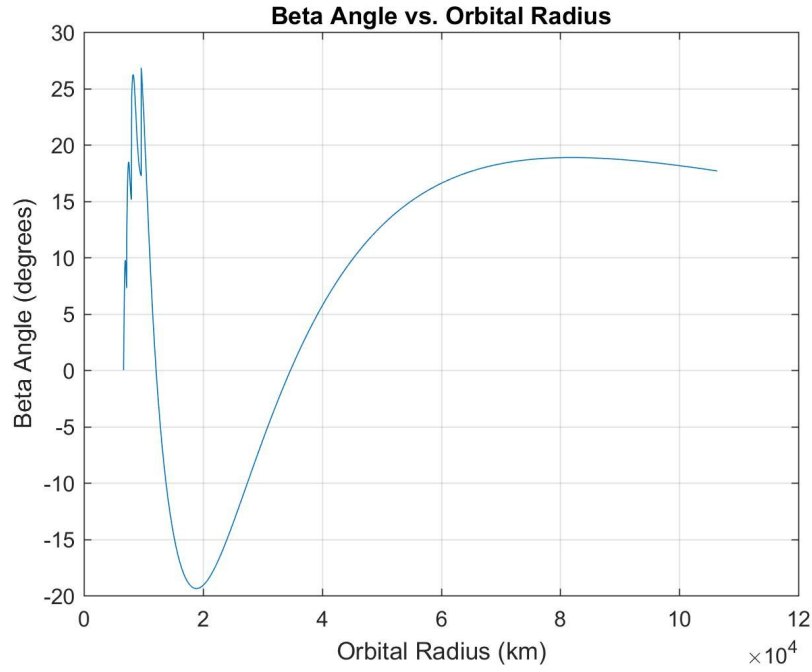The eclipse fraction represents the fraction of an orbital period that the craft will be in eclipse.
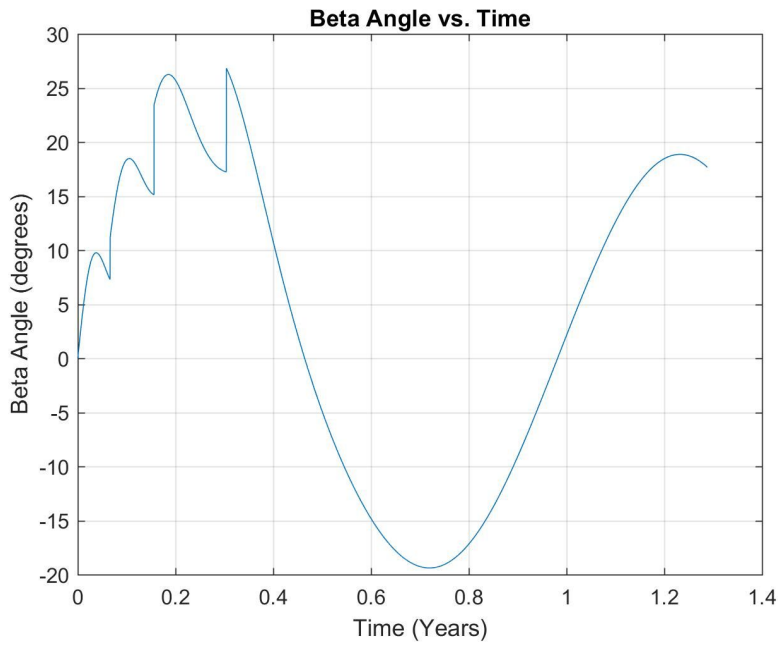

Fig. 15   Beta Angle vs. Orbital Radius.

Fig. 16   Beta Angle vs. Transfer Time.

39

Figures 15 and 16 show the change in the Beta angle over the course of the craft's orbit transfer. The angle remains bounded within ± 28.59 degrees, as predicted above. As the craft's orbital radius increases, the frequency of Beta's oscillations decrease.
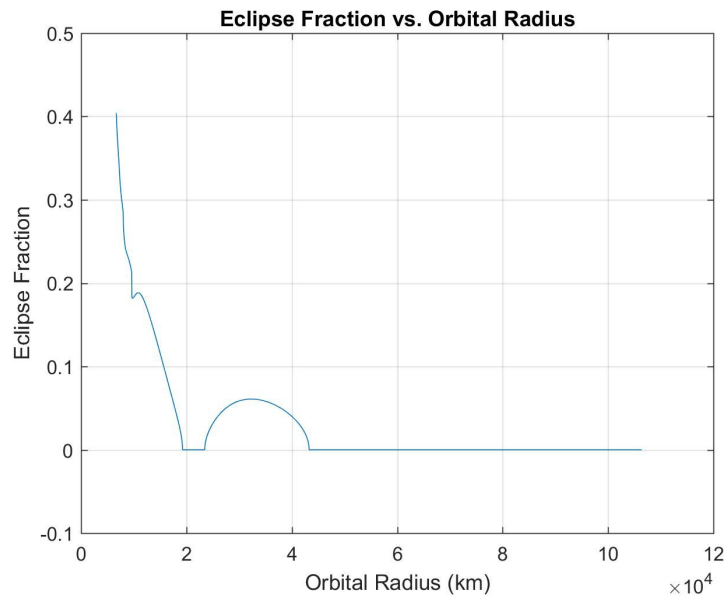

Fig. 17   Eclipse Fraction vs. Orbital Radius.
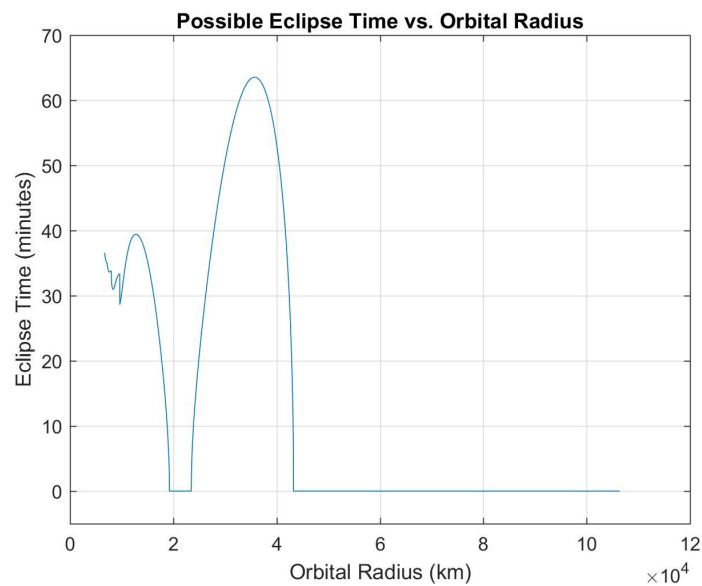

Fig. 18   Possible Eclipse Time vs. Orbital Radius.

Figure 18 shows the craft's eclipse fraction over the course of its transfer spiral. The fraction starts close to 0.4 in LEO and quickly drops to zero by the time the craft's orbital radius has increased to 20,000 km, with a slight increase happening while the craft is in geostationary space. The calculated eclipse fraction and eclipse time in geostationary space matches the values known from [28]. Note that while some variation in the timing of these calculations is possible depending on what time of year the craft begins its transfer maneuver, the eclipse fraction

will always be largest in LEO, and any eclipse that can occur while the craft is past geostationary space is highly unlikely and infrequent, about to the tune of total lunar eclipses.

Figure 18 shows that the maximum eclipse time the craft will experience is about an hour in GEO space, and about 35-40 minutes in LEO. This maximum eclipse time in GEO dictates the overall capacity of the batteries, but the eclipses only happen in the off chance that the craft is passing through GEO space during the fall or spring equinox. The higher frequency of eclipses in LEO necessitate a power schedule that can keep the batteries sufficiently charged during the craft's short times in the Sun. This power schedule will start with a larger fraction of the power generated being used to charge the batteries, and slowly lower that fraction proportionally to the eclipse fraction.

B. Xenon Propellant Sourcing & The Environment

At 6,000 kg per cycle, SPrIntR will require a larger yearly Xenon propellant load than has ever been expended on a singular space mission. It is therefore imperative to examine the current Xenon market and make predictions on the future trends of worldwide Xenon production. As of 2015, the annual worldwide production of Xenon was estimated to be 53,000 kg [29]. A 6,000 kg purchase of Xenon would account for about 11% of this annual production rate. From the same source, it is estimated that Xenon makes up about 0.000009% of the Earth's atmosphere, making for a total of $2x10^{12}$ kg. Even with the Mars phase SPrIntR's yearly propellant needs of about 15,000 kg per year, there is enough Xenon in the atmosphere to supply the mission for 133 million years, however, care must be taken in purchasing the gas over several years in increasing quantities, allowing the market to adjust to the new demand and avoiding a dramatic spike in the price of the gas. Over the past 40 years, the supply world supply of Xenon has grown more than 10-fold [48], and this trend is likely to continue due to the rapidly increasing adoption of electric propulsion systems for satellites and other spacecraft. With the market predicted to continue expanding in this way, acquiring the necessary propellant for SPrIntR missions is within the realm of possibility and reason.

C. Assembly in LEO

Aggregation and assembly of SPrIntR's vehicle components will take place in LEO which has a assembly time requirement of less than 60 days. Attention has been given to packaging for launch for the least number of launches. With the current structural design of SPrIntR, it is estimated that the first incarnation will be able to be entirely stow in the Delta IV Heavy 5m cargo fairing, preempting the need for assembly in LEO. The Mars SPrIntR is able to be entirely stow in the SLS Block 2B cargo fairing. At a maximum, the Mars SPrIntR may need two launches, which still satisfies the top-level requirements, due to the communications array being 3m in diameter.

The launch vehicle that will carry the lunar SPrIntR into LEO is the Delta IV heavy. Other launch vehicles were analyzed such as the Falcon 9, SLS, and the Atlas V. All of those launch vehicles could not reach LEO with a fully assembled SPrIntR onboard. The SLS has a minimum payload of 30000 kg, a wet SPrIntR without the payload is roughly 17488 kg. Thus, it would be inefficient and unlikely that a SLS would be acquired for this mission. The Atlas V doesn't have the payload capacity to carry SPrIntR to LEO, but it's fairing dimensions are satisfactory. The Falcon 9 Heavy has a payload liftoff mass which can carry the wet SPrIntR, but it's fairing options are to small at this time. [14]

The SPrIntR needs to stow its solar arrays when inside of the fairing. The two configuration for the stowed solar arrays can be seen in Figure 19.

Fig. 19 SPrIntR Configurations.

41

The configurations on the left (config. type I) of Figure 19 shows a SPrIntR with its solar arrays stowed forward, this configuration allows for the smallest footprint of the two configurations but has the largest length of 10 meters. The second configuration (config. type II) has the largest footprint but the smallest length. Config. type II has a length of 9m and a footprint of 6x3.65m.

Config. type II requires more volume within a fairing but has an advantageous attachment method via the docking ring. While config. type I must have a custom adapter which will clamp onto the engine flange, thus adding more mass to the launch. Config. type I was selected because the Delta V Heavy has a max fairing size of 5m, thus config. type II would not fit within the fairing. Therefore, config. type I was selected. The Delta V Heavy was chosen because it has a 5m diameter fairing with a length of 19.1m (Delta IV H Long Fairing). This ensured the SPrIntR had enough room for the stowed solar arrays. The engine plate did have to be circularized at the edges to fit into the 5m fairing with a 5.1 cm tolerance between the fairing and SPrIntR [14].

The fairing will fit the Lunar SPrIntR but an adapter must be custom made to attach the SPrIntR safely. This adapter will bolt onto the Delta IV 4293-5 PAF adapter. Once bolted it will attach to the SPrIntR via the engine flanges. These flanges will be mechanically clamped into a slot on the custom adapter, once the desired altitude is reached these adapter clamps will release the SPrIntR. The adapter will then stay with the fairing and fall back to earth, The custom adapter is made from aluminum and has a mass of 5500 kg. This brings the total liftoff mass of the SPrIntR assembly to 22988 kg which is below the maximum LEO liftoff mass of 26000 kg.

D. 500 kW Mars Extensibility

As per the requirements set by the mandate, the SPrIntR design must be extensible for a 500 kW Mars mission variant. The 500 kW SPrIntR has the same bus geometry with slight variations. The engine array that is on the 200 kW SPrIntR variant will be enlarged from 25 NEXT thrusters to 65 NEXT thrusters, this will ensure that the additional power can be used for propulsion. To achieve an extra 300 kilowatts of power, the two existing 21 m Megaflex solar panels will be replaced with 32 meters variants.

The same analysis using ANSYS, which was used for the Lunar SPrIntR, was used for the Mars SPrIntR. Due to the increase of the payload size and mass of the subsystems, every aspect of the SPrIntR's structure was thickened, and the size of the SPrIntR was enlarged. The main bus of the SPrIntR was enlarged to an area of 4x4 meters and the exterior bus wall thickened to 6.5mm. Additionally, the docking ring has increased to 32.63 kg. The central carbon fiber cylinder has a thickness of 3.5cm and is now 3m in diameter. The back plate and engine flanges have increased to a thickness of 4.5cm and 2.6cm, respectively. The engine base plate has an area of 5.6x5.6m, due to the 65 NEXT thrusters. The Mars SPrIntR has a total structural mass of 7399 kg which is a 190% increase from the Lunar SPrIntR

The extensible SPrIntR, like the Lunar SPrIntR will not have an assembly plan in LEO due to the SLS Block 2B's fairing size. The Mars SPrIntR cannot fit into the Block 1B because the 5.6x5.6m engine plate; to fit, the SPrIntR must drop the thruster count from 65. In addition, a custom flange adapter must to be designed to ensure the safety of the SPrIntR's thruster array during launch.

Due to the distance of Mars, the temperature of the bus will drop underneath the design limitations of critical components. In contrast, the power portion of the bus must have a larger radiator to extract heat solely from the PPU's. The radiator must be 51.51 m^2 to accomplish this task. NASA typical wants areal densities for radiators to be between 2-4 kg/m^2 therefore the mass for the Mars mission radiator will be approximately 105 kg.

As discussed previously, the Mars phase SPrIntR will have a payload capacty of 24,000 kg, and a required propellant load of 31,000 kg per cycle. With these parameters, one cycle will take approximately 2.6 years.

E. Component Replacement

The components with the shortest lifespan and most likely to fail are the NEXT gridded ion thrusters and the lithium-ion batteries, as well as some power system components such as diodes or switches. The thrusters have a lifetime of at least 55,000 hours[5], and the batteries have a cycle life of about 15,000 cycles, which corresponds to about 10 years. Each will need to be replaced at some point in the life of the mission. At the end of thruster or battery life, or component failure, SPrIntR will rendezvous and dock with either the ISS or a crewed orbital craft, where astronauts can perform replacement EVAs. Component replacement is more cost efficient than reconstructing another SEP tug.

V. Conclusions

As humans turn their sights to the stars in the pursuit of knowledge and possibly a new home, NASA has advanced plans to place a space station in orbit around the moon. This station would serve as a base for scientific observation and staging activities for human excursions to deep space, and would need to be periodically resupplied. With the prohibitive costs of surface launch vehicles, especially for destinations further than Low Earth Orbit, it becomes necessary to analyze the potential for alternative payload transportation methods. Advances in solar power generation and electric propulsion technologies allows for payloads to be transported using relatively small amounts of propellant compared to traditional launch vehicles. The design for a 200 kW solar-electric-propulsion space cargo ship has been presented. This cargo ship will ferry payloads from LEO to LDRO and back, and the design is extensible to 500 kW for deep space excursions to Mars and beyond. This review is submitted as documentation and justification of the design decisions made thus far regarding mission architectures, requirements, and subsystems.

A. Future Design Considerations

1. Extensibile SPrIntR Communication Attachment

The extensibile SPrIntR must have communication availability at a five sol orbit around Mars. The communications subsystem requires a 3m diameter parabolic antenna to accomplish this task. This antenna will cause interference problems within the SLS Block 2B if it is mounted onto the side of SPrIntR's bus, and it cannot stow internally due to its size. Therefore, future work must be conducted to design an attachment method for the antenna to sit on the front of the SPrIntR's bus via an adjustable arm. If this design is infeasible, then multiple launches must take place to attach the antenna to SPrIntR.

2. Radiation Shielding

SPrIntR must travel from LEO to LDRO to drop of its payload. SPrIntR will inevitably spend a large portion of its time within the inner and outer radiation belt between the Earth and the Moon. Therefore, SPrIntR must have sufficient shielding for all major subsystems within the bus for long periods of radiation exposure. The radiation shielding will be an extra layer of metal alloy around the subsystem which will add to the structural weight. This will be very similar to the MMOD sacrificial plates. This analysis will be taken into consideration during the next structures iteration cycle.

3. Communication Internal Stowage (Lunar SPrIntR)

The compacted Megaflex solar arrays will stow in a forward position as in Figure (). This will cause the arrays to interact with the communications antenna; therefore, an internal stowage compartment must be designed. The antenna will sit on a small track system which is attached to several motors inside of the bus. When the SPrIntR is inside of the Delta IV Heavy fairing, this system will house the antenna and ensure its structural stability. Once the Megaflex solar arrays are deployed in LEO, the motors will deploy the antenna to the outside SPrIntR wall.

4. Modeling Propellant Feed Lines

Due to time constraints, the design and modeling of the propellant feed lines was not accomplished. In the future, the feed liens will be sized and placed in an optimal manner behind the insulation wall in the back end of the bus. This will also be shown in a finalized CAD model.

5. Design Ammonia Cooling System

The size of the radiator has been designed to ensure the heat within the bus is extracted, but do to uneven radiator heating, an ammonia cooling system must be designed. This system will include a pump, lines, cold plates, and fixtures. This will allow for excess heat to be evenly distributed to the outer radiator array panels, therefore causing optimal heat dissipation to occur. This system must be redesigned for the extensible SPrIntR because the power subsystem becomes too hot while the other subsystems drop below their operating temperatures. Therefore, the ammonia lines will run from the power subsystem into the other subsystems to replace the need of a heater. This design will be based off of Boeing's cooling system [15].

6. Completed GMAT Trajectories for Lunar and Mars Mission

The current public version of GMAT (R2017a) does not have a built-in optimizer. This is due to legal reasons involving NASA's open-source code used on GMAT. Because of this trajectory design is severely hindered for electric propulsion, which will require optimizing using multiple shooting and patch points. The next release of GMAT (R2018a) will have a built-in optimizer. It will then be vastly easier to design the low-thrust trajectory needed for SPrIntR. Through communication with individuals involved in the GMAT developing, the new version was supposed to be release in March 2018. This did not happen and the release date has been pushed further, and thus will not be able to help the SPrIntR trajectory design.

7. SADA Harness Design

The current solar array drive is the C50 Incremental Rotary Actuator from Sierra Nevada Corporation. This does not actually transmit the power generated from the solar arrays and therefore an actual solar array drive assembly (SADA) will need to be used.

8. Power System Component Selection

In the future, more detailed and specific power system component selection and trade studies need to take place. This would include selecting things like power converters, controllers, sensors, fuses, diodes, and switches.

References

[1] Wertz, J., Everett, D., Puschell, J., "Space Mission Engineering: The New SMAD", Microcosm Press, 2015

[2] E. Stuhlinger, Ion Propulsion for Space Flight, Mc Graw Hill Book Co., New York, 1964

[3] R. G. Jahn, Physics of Electric Propulsion, Dover Publications Inc., New York, 1968.

[4] Orbital ATK UltraFlex™ Fact Sheet.
    URL: https://www.orbitalatk.com/space-systems/space-components/solar-arrays/docs/UltraFlex_Factsheet.pdf

[5] Sovey, J.S., Soulas, G.C., Herman, D.A. (NASA Glenn Research Center). May 01, 2011. "NEXT Propellant Management System Integration With Multiple Ion Thrusters". NTRS. https://ntrs.nasa.gov/search.jsp?R=20110012903

[6] Welles, R.P. (The Aerospace Corporation), "Propellant Storage Considerations for Electric Propulsion". *proceedings of the 22nd International Electric Propulsion Conference*. 199

[7] Sierra Nevada Actuators
    http://mediakit.sncorp.com/mediastore/document/Space-Technologies-Product-Catalog.pdf

[8] United Launch Alliance, "Delta IV Launch Vehicle Services User Guide", ULA Inc., June 2013,
    https://www.ulalaunch.com/docs/default-source/rockets/delta-iv-user%27s-guide.pdf

[15] IDS Business Support, "Active Thermal Control System Overview", Boeing, 2018,
    https://www.nasa.gov/pdf/473486main_iss_atcs_overview.pdf

[9] Stowed UltraFlex™ and MegaFlex™
    URL: https://www.nasa.gov/offices/oct/home/feature_sas.html

[10] CMG Data Sheet
    URL: http://www2.l3t.com/spacenav/pdf/datasheets/CMG.pdf.

[11] Monopropellant Thruster Data Sheet.
    URL:
    http://www.moog.com/literature/Space_Defense/Spacecraft/Propulsion/Monopropellant_Thrusters_Rev_0613.pdf.

[12] Janschek, Klaus. "ESA Guidance, Navigation, and Control Systems," Technische Universitat Dresden. January 2014. URL:
    http://www.et.tu-dresden.de/ifa/fileadmin/user_upload/www_files/Aktuelles/2014-01-27_ESA_Guidance__Navigation__and_Control_Systems.pdf

[13] Northrop Grumman LN-200S Data Sheet. URL:
    http://www.northropgrumman.com/Capabilities/LN200FOG/Documents/ln200s.pdf

[14] Space Micro MSS-01,02 Data Sheet. URL: https://www.spacemicro.com/assets/datasheets/guidance-and-nav/MSS.pdf

[15] Sodern HYDRA-M Data Sheet. URL:
    http://www.sodern.com/website/docs_wsw/RUB_215/tile_508/Datasheet_HYDRA_M_2017.pdf

[16] Larson, W., Wertz, J.. "Space Mission Analysis and Design: Third Edition", Microcosm Press, 2005

[17] L3 Travelling Wave Tube Amplifiers. URL: http://www2.l3t.com/edd/pdfs/datasheets/TWT%20Overview.pdf

[18] Skyware Technologies Value Enterprise Ka-Band VSAT Transceiver.
    URL: http://www.skywaretechnologies.com/images/documents/pdf/XRC33F16CD.pdf

[19] Microsemi Voltage Controlled Gunn Oscillator.
    URL: https://www.microsemi.com/document-portal/doc_view/122458-msc-gunn-oscillators-vco-pdf

[20] Antesky Space Technology Inc. 2015. http://www.antesky.com/project/3meter-satellite-dish-vsat-antenna/

[21] Poole, I. "Parabolic Reflector Antenna Gain", Radio-Electronics.com. Accessed: March 22, 2018.
   URL: http://www.radio-electronics.com/info/antennas/parabolic/parabolic-reflector-antenna-gain.php

[22] Casas, Ed. "Link Budget Calculations and Final Review", The University of British Columbia, 2000. Accessed: March 22, 2018. URL: http://www.ece.ubc.ca/~edc/563/lectures/lec10.pdf

[23] Gilmore, David G. Spacecraft Thermal Control Handbook. Aerospace Press, 2002.

[24] Tomboulian, B. "Lightweight, High-Temperature Radiator for In-Space Nuclear-Electric Power and Propulsion", scholarworks.umass.edu. Accessed: March 30, 2018.
   URL: https://scholarworks.umass.edu/cgi/viewcontent.cgi?referer=https://www.google.com/&httpsredir=1&article=1217&context=dissertations_2

[25] http://webserver.dmt.upm.es/~isidoro/tc3/Radiation%20View%20factors.pdf

[26] http://www.qrg.northwestern.edu/projects/vss/docs/thermal/2-what-temperature-is-the-engine.html

[27] Rickman, S. L., "Introduction to On-Orbit Thermal Environments," NASA NESC Academy.

[28] "Eclipse Seasons" Intelsat.
   URL:
   http://www.intelsat.com/tools-resources/library/satellite-101/eclipse-seasons/

[29] Herman, D.A., Unfried, K.G. (NASA Glenn Research Center). 2015. "Xenon Acquisition Strategies for High-Power Electric Propulsion NASA Missions". NTRS. https://ntrs.nasa.gov/search.jsp?R=20150023080